Metabolic Flux Analysis of Plastidic Isoprenoid Biosynthesis in Poplar Leaves Emitting and Nonemitting Isoprene[1][W]

Andrea Ghirardo, Louwrance Peter Wright, Zhen Bi, Maaria Rosenkranz, Pablo Pulido, Manuel Rodríguez-Concepción, Ülo Niinemets, Nicolas Brüggemann, Jonathan Gershenzon, and Jörg-Peter Schnitzler*

Research Unit Environmental Simulation, Institute of Biochemical Plant Pathology, Helmholtz Zentrum München, 85764 Neuherberg, Germany (A.G., Z.B., M.R., J.-P.S.); Department of Biochemistry, Max Planck Institute for Chemical Ecology, 07745 Jena, Germany (L.P.W., J.G.); Centre for Research in Agricultural Genomics (CRAG), CSIC-IRTA-UAB-UB, 08193 Barcelona, Spain (P.P., M.R.-C.); Institute of Agricultural and Environmental Sciences, Estonian University of Life Sciences, 51014 Tartu, Estonia (Ü.N.); and Institute of Bio- and Geosciences-Agrosphere (IBG-3), Forschungszentrum Jülich, 52425 Juelich, Germany (N.B.)

The plastidic 2-C-methyl-D-erythritol-4-phosphate (MEP) pathway is one of the most important pathways in plants and produces a large variety of essential isoprenoids. Its regulation, however, is still not well understood. Using the stable isotope ^{13}C-labeling technique, we analyzed the carbon fluxes through the MEP pathway and into the major plastidic isoprenoid products in isoprene-emitting and transgenic isoprene-nonemitting (NE) gray poplar (*Populus* × *canescens*). We assessed the dependence on temperature, light intensity, and atmospheric [CO_2]. Isoprene biosynthesis was by far (99%) the main carbon sink of MEP pathway intermediates in mature gray poplar leaves, and its production required severalfold higher carbon fluxes compared with NE leaves with almost zero isoprene emission. To compensate for the much lower demand for carbon, NE leaves drastically reduced the overall carbon flux within the MEP pathway. Feedback inhibition of 1-deoxy-D-xylulose-5-phosphate synthase activity by accumulated plastidic dimethylallyl diphosphate almost completely explained this reduction in carbon flux. Our data demonstrate that short-term biochemical feedback regulation of 1-deoxy-D-xylulose-5-phosphate synthase activity by plastidic dimethylallyl diphosphate is an important regulatory mechanism of the MEP pathway. Despite being relieved from the large carbon demand of isoprene biosynthesis, NE plants redirected only approximately 0.5% of this saved carbon toward essential nonvolatile isoprenoids, i.e. β-carotene and lutein, most probably to compensate for the absence of isoprene and its antioxidant properties.

Isoprenoids represent the largest and most diverse group (over 50,000) of natural compounds and are essential in all living organisms (Gershenzon and Dudareva, 2007; Thulasiram et al., 2007). They are economically important for humans as flavor and fragrance, cosmetics, drugs, polymers for rubber, and precursors for the chemical industry (Chang and Keasling, 2006). The broad variety of isoprenoid products is formed from two building blocks, dimethylallyl diphosphate (DMADP) and isopentenyl diphosphate (IDP). In plants, the plastidic 2-C-methyl-D-erythritol-4-phosphate (MEP) pathway (Zeidler et al., 1997) produces physiologically and ecologically important volatile organic compounds (VOCs), the carotenoids (tetraterpenes; Giuliano et al., 2008; Cazzonelli and Pogson, 2010), diterpenes, the prenyl side-chains of chlorophylls (Chls) and plastoquinones, isoprenylated proteins, the phytohormones gibberellins, and side-chain of cytokinins (for review, see Dudareva et al., 2013; Moses et al., 2013). Industrially important prokaryotes (e.g. *Escherichia coli*) also use the MEP pathway for the biosynthesis of isoprenoids (Vranová et al., 2012), and there is an increasing interest in manipulating the MEP pathway of engineered microbes to increase production of economically relevant isoprenoids (Chang and Keasling, 2006). To achieve this, a mechanistic understanding of the regulation of the MEP pathway is needed (Vranová et al., 2012).

Some plants, including poplars (*Populus* spp.), produce large amounts of the hemiterpene VOC isoprene. Worldwide isoprene emissions from plants are estimated

[1] This work was supported by the Human Frontier Science Program (to J.-P.S. and Ü.N.), the Deutsche Forschungsgemeinschaft (grant no. SCHN653/4–3), the Spanish Ministry of Science and Innovation (grant nos. IUPAC/PIM2010IPO–00660 and BIO2011–23680), the Estonian Ministry of Science and Education (institutional grant no. IUT–8–3 to Ü.N.), the Estonian Science Foundation (grant no. 9253 to Ü.N.), and a Max Planck-Fraunhofer collaboration grant (to L.P.W).

* Address correspondence to jp.schnitzler@helmholtz-muenchen.de.

The author responsible for distribution of materials integral to the findings presented in this article in accordance with the policy described in the Instructions for Authors (www.plantphysiol.org) is: Jörg-Peter Schnitzler (jp.schnitzler@helmholtz-muenchen.de).

[W] The online version of this article contains Web-only data.

www.plantphysiol.org/cgi/doi/10.1104/pp.114.236018

to be 600 teragrams per year and to account for one-third of all hydrocarbons emitted to the atmosphere (Arneth et al., 2008; Guenther, 2013). Isoprene has strong effects on air chemistry and climate by participating in ozone formation reactions (Fuentes et al., 2000), by prolonging the lifespan of methane, a greenhouse gas (Poisson et al., 2000; Archibald et al., 2011), and by taking part in the formation of secondary organic aerosols (Kiendler-Scharr et al., 2012).

Poplar leaves invest a significant amount of recently fixed carbon in isoprene biosynthesis (Delwiche and Sharkey, 1993; Schnitzler et al., 2010; Ghirardo et al., 2011) to cope with abiotic stresses (Sharkey, 1995; Velikova and Loreto, 2005; Behnke et al., 2007, 2010b, 2013; Vickers et al., 2009; Loreto and Schnitzler, 2010; Sun et al., 2013b), although there are indications that other protective mechanisms can partially compensate the lack of isoprene emission in genetically transformed poplars (Behnke et al., 2012; Way et al., 2013). It has been suggested that in isoprene-emitting (IE) species, most of the carbon that passes through the MEP pathway is used for isoprene biosynthesis (Sharkey and Yeh, 2001). However, a recent study using pulse-chase labeling with ^{14}C has shown continuous synthesis and degradation of carotenes and Chl *a* in mature leaves of Arabidopsis (*Arabidopsis thaliana*; Beisel et al., 2010), and the amount of flux diverted to carotenoid and Chl synthesis compared with isoprene biosynthesis in poplar leaves is not known.

Isoprene emission is temperature, light, and CO_2 dependent (Schnitzler et al., 2005; Rasulov et al., 2010; Way et al., 2011; Monson et al., 2012; Li and Sharkey, 2013a). It has been demonstrated that isoprene biosynthesis depends on the activities of IDP isomerase (EC 5.3.3.2), isoprene synthase (ISPS; EC 4.2.3.27), and the amount of ISPS substrate, DMADP (Brüggemann and Schnitzler, 2002a, 2002b; Schnitzler et al., 2005; Rasulov et al., 2009b). In turn, DMADP concentration has been hypothesized to act as a feedback regulator of the MEP pathway by inhibiting 1-deoxy-D-xylulose-5-phosphate synthase (DXS; EC 2.2.1.7), the first enzyme of the MEP pathway (Banerjee et al., 2013). Understanding the controlling mechanism of isoprene biosynthesis is not only of fundamental relevance, but also necessary for engineering the MEP pathway in various organisms and for accurate simulation of isoprene emissions by plants in predicting atmospheric reactivity (Niinemets and Monson, 2013).

There is ample evidence that silencing the ISPS in poplar has a broad effect on the leaf metabolome (Behnke et al., 2009, 2010a, 2013; Way et al., 2011; Kaling et al., 2014). While some of those changes (e.g. ascorbate and α-tocopherol) are compensatory mechanisms to cope with abiotic stresses, others (e.g. shikimate pathway and phenolic compounds) might be related to the alteration of the MEP pathway (Way et al., 2013; Kaling et al., 2014). The perturbation of these metabolic pathways can be attributed to the removal of a major carbon sink of the MEP pathway and the resulting change in the energy balance within the plant cell (Niinemets et al., 1999; Ghirardo et al., 2011). In this work, we analyzed the carbon fluxes through the MEP pathway into the main plastidic isoprenoid products.

We used the ^{13}C-labeling technique as a tool to measure the carbon fluxes through the MEP pathway at different temperatures, light intensities, and CO_2 concentrations in mature leaves of IE and transgenic, isoprene-nonemitting (NE) gray poplar (*Populus* × *canescens*). Isoprene emission was drastically reduced in the transgenic trees through knockdown of *PcISPS* gene expression by RNA interference, resulting in plants with only 1% to 5% of isoprene emission potential compared with wild-type plants (Behnke et al., 2007).

We measured the appearance of ^{13}C in the isoprenoid precursors 2-C-methyl-D-erythritol-2,4-cyclodiphosphate (MEcDP) and DMADP as well as isoprene and the major downstream products of the MEP pathway, i.e. carotenoids and Chls. To reliably detect de novo synthesis of the pigments, which occur at very low rates (Beisel et al., 2010), we used isotope ratio mass spectrometry (IRMS).

Here, (1) we quantify the effect of isoprene biosynthesis on the MEP pathway in poplar, and (2) we show that suppression of isoprene biosynthesis negatively affects the carbon flux through the MEP pathway by accumulating plastidic DMADP, which feeds back to inhibit PcDXS, leading to (3) a slight increase of carbon flux toward production of greater chain-length isoprenoids and (4) a strong decrease in the overall isoprenoid carbon fluxes to compensate for the much lower MEP pathway demand for carbon. This study strongly supports the hypothesis that an important regulatory mechanism of the MEP pathway is the feedback regulation of plastidic DMADP on DXS. The large carbon flux through the MEP pathway of IE poplar plastids demonstrates the potential of transgenically altered IE plant species to produce economically valuable isoprenoids at high rates in, for instance, industrial applications.

RESULTS

^{13}C-Labeling Pattern of MEcDP, DMADP, and Isoprene upon $^{13}CO_2$ Feeding

Upon illumination, $^{13}CO_2$ was rapidly incorporated into intermediates and products of the MEP pathway. The isotopic ^{13}C composition of the intermediate MEcDP was similar to the isotopic composition of emitted isoprene from illuminated IE and NE mature leaves but differed from the isotopic composition of total DMADP (Fig. 1, A–C). The isotopic ^{13}C pattern of the pathway product DMADP was different between IE and NE leaves ($P < 0.001$, ANOVA), the latter having a larger proportion of fully (C_5) labeled DMADP and a smaller fraction of unlabeled DMADP (Fig. 1B). In similar experiments followed by 1 h of darkness, the ^{13}C patterns of MEcDP and isoprene again correlated with each other but not with the pattern of DMADP (Fig. 1, A–C).

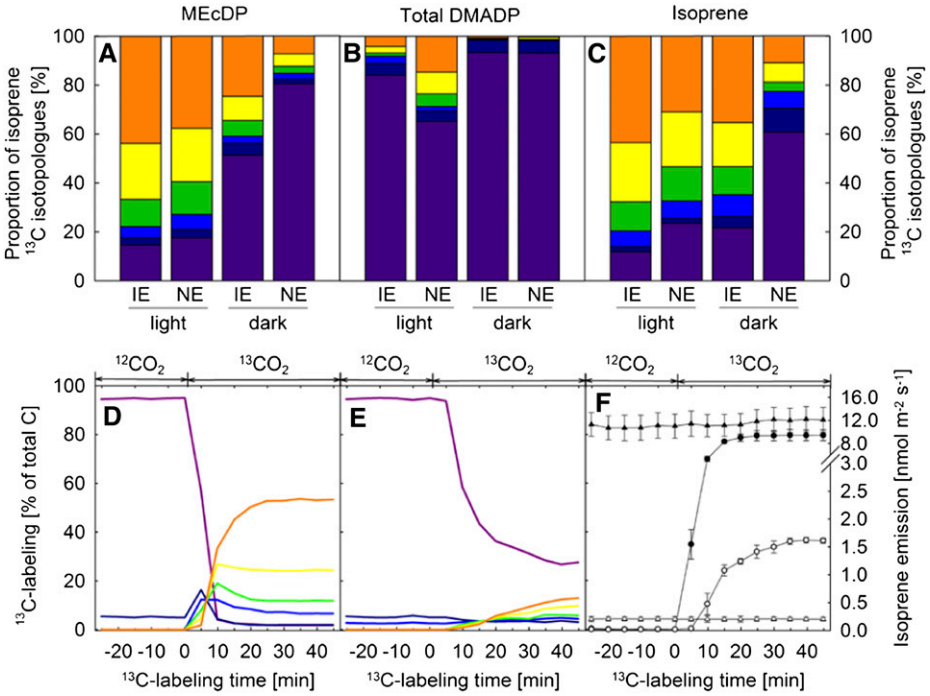

Figure 1. Isotopic ^{13}C composition of MEcDP (A), total (plastidic and nonplastidic) DMADP (B), and isoprene (C) after feeding leaves for 45 min with 380 μmol mol^{-1} $^{13}CO_2$ in experiments under controlled environmental conditions with 1 h and 45 min of illumination (PPFD = 1,000 μmol m^{-2} s^{-1}) and in experiments with illumination followed by 1 h of darkness (PPFD = 0; kept under $^{13}CO_2$; leaf temperature = 30°C). Dynamics of ^{13}C incorporation into isoprene in IE (D) and NE (E) leaves and incorporation rate of ^{13}C into isoprene in IE (black circle) and NE (white circle) leaves and associated isoprene emission rates (F; black triangles, IE; white triangles, NE) under light condition. The isotopologue masses of MEcDP, DMADP, and isoprene are shown using different colors, representing the incorporation of different numbers of ^{13}C-labeled carbon atoms: purple, $^{13}C_0$; dark blue, $^{13}C_1$; light blue, $^{13}C_2$; green, $^{13}C_3$; yellow, $^{13}C_4$; and orange, $^{13}C_5$). Shown are means (±SE) of four biological replicates.

Online measurements of isotopologue masses of isoprene showed that under a $^{13}CO_2$ atmosphere, NE leaves incorporate a lower proportion of ^{13}C into isoprene than IE leaves (Fig. 1, D and E; $P < 0.001$), reaching a maximum ^{13}C incorporation of approximately 40% after 40 min (Fig. 1E). By contrast, IE leaves reached 80% ^{13}C incorporation within 15 min. Taken together, the ^{13}C isotopic analysis of isoprene and two of its intermediates was a clear indication of differences in the MEP pathway of NE and IE leaves.

Cellular Distribution of DMADP in IE and NE Plants

We utilized the fast incorporation of freshly assimilated $^{13}CO_2$ into isoprene and the corresponding MEP pathway metabolites to measure the cellular distribution of DMADP within the plastidic and nonplastidic pools (Ghirardo et al., 2010a). Silencing of PcISPS resulted in an enormous accumulation of plastidic DMADP in NE compared with that in IE leaves ($P < 0.001$; Fig. 2).

Under standard conditions (incident photosynthetically active quantum flux density [PPFD] of 1,000 μmol m^{-2} s^{-1}, leaf temperature of 30°C, CO_2 concentration of 380 μmol mol^{-1}), NE leaves showed a much larger plastidic DMADP pool (36.2 ± 2.0 μmol m^{-2}) compared with illuminated IE leaves (1.42 ± 0.22 μmol m^{-2}) and also a much larger relative partition into plastids, 94% ± 3% of the total DMADP content. In IE leaves, 15% ± 2% of the DMADP was partitioned in the plastidic pool, which was significantly ($P < 0.001$) depleted after 1 h of darkness, whereas nonplastidic DMADP remained unaffected.

Temperature, Light, and CO_2 Dependencies of MEcDP and Plastidic DMADP Pools

The MEP pathway intermediate MEcDP was depleted in NE compared with IE leaves, under different environmental conditions (Fig. 3, A, C, and E). Among the different environmental conditions, IE leaves showed the strongest accumulation of MEcDP and plastidic DMADP under 30°C leaf temperature, PPFD of 1,000 μmol photons m^{-2} s^{-1} and ambient CO_2 concentration of 380 μmol mol^{-1}. The strongest significant differences with lowest P value between IE and NE lines were found in the MEcDP content at 35°C ($P < 0.001$, ANOVA) and in the plastidic DMADP content at a PPFD of 100 μmol m^{-2} s^{-1} ($P < 0.001$, ANOVA). In

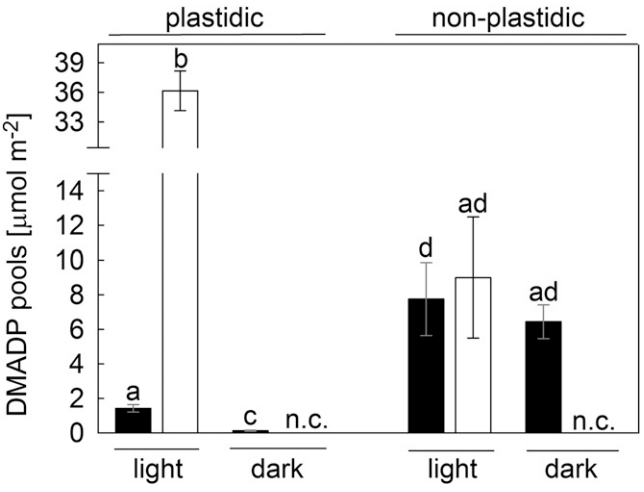

Figure 2. Calculated plastidic and nonplastidic DMADP pools in illuminated IE (black) and NE (white) leaves (acclimated at 1,000 μmol m^{-2} s^{-1} of incident PPFD, 30°C leaf temperature, and 380 μmol mol^{-1} of CO_2) and in experiments followed by 1 h of darkness (PPFD = 0). Means of $n = 4 \pm$ SE. Significant differences at $P < 0.01$ are denoted by different letters (one-way ANOVA with Tukey's test). n.c., Not calculated due to nondetectable isoprene emission.

IE leaves, the MEcDP pool size correlated well with the pool size of plastidic DMADP at all different environmental conditions (Fig. 3). The only exception was at the highest temperature (40°C), where the pool of MEcDP sharply decreased relative to DMADP. By increasing temperature from 25°C to 40°C, we observed a rapid increase of both pools up to 30°C, followed by a gradual decrease at temperatures higher than 30°C (Fig. 3, A and B). Light dependency revealed a steep increase of the MEcDP and plastidic DMADP pools between 250 and 1,000 μmol m^{-2} s^{-1} PPFD (Fig. 3, C and D). By contrast, the increase of CO_2 concentration negatively affected the accumulation of MEcDP and plastidic DMADP compounds (Fig. 3, E and F). In NE leaves, increasing temperature negatively affected the plastidic DMADP pool ($P < 0.05$), although different light intensities and CO_2 concentrations did not (Fig. 3B). Overall, the plastidic pool of DMADP was always much larger in NE compared with IE, except at 40°C, where the temperature stress reduced the plastidic pool of DMADP, and the pool sizes were not statistically different between the leaves of NE and IE poplar ($P = 0.57$, ANOVA). Therefore, suppression of isoprene biosynthesis resulted in alteration of isoprenoid precursor pools, with higher content of plastidic DMADP and lower content of MEcDP in NE relative to IE plants.

Effects of in Vivo Plastidic DMADP Pools on in Vitro PcDXS Activities

In vitro PcDXS activities, measured under saturated substrate concentrations, differed significantly between IE and NE (Fig. 4A; $P < 0.01$, ANOVA). Apparent PcDXS activity in NE leaf extracts was approximately 55% lower than the PcDXS activity of IE leaves, indicating that the much greater reduction in metabolic flux (see section below) in NE plastids is not triggered by a comparable reduction of apparent DXS activity. This coincides to a certain extent with the analysis of gene transcript levels. Neither the expression of MEP pathway (*PcDXS*, *1-deoxy-D-xylulose-5-reductoisomerase* [*PcDXR1*], *PcDXR2*, *diphosphocytidyl methylerythritol kinase* (*PccMK*), and *4-hydroxy-3-methylbut-2-en-1-yl diphosphate reductase* (*PcHDR*)) nor mevalonate (MVA) pathway (*3-hydroxy-3-methylglutaryl CoA reductase* (*PcHMGR*) and *MVA kinase* (*PcMEV*) genes differed significantly between IE and NE plants (Supplemental Fig. S1).

Because enzymatic activity and transcript levels suggested that posttranscriptional mechanisms may influence in vivo PcDXS activity, we explored the

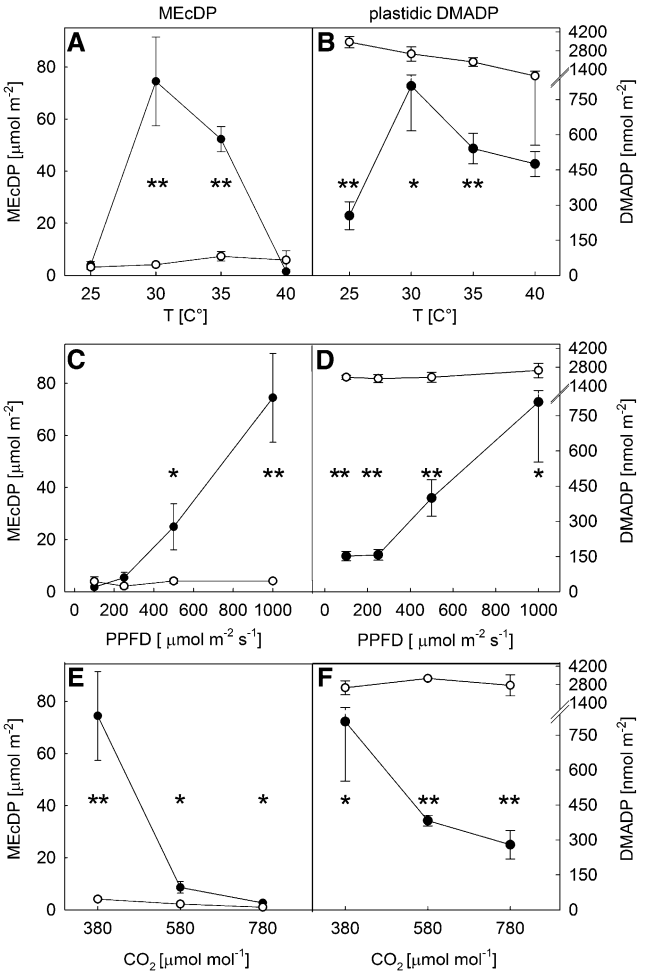

Figure 3. Temperature (A and B), light (C and D), and CO_2 (E and F) dependencies of MEcDP (left) and plastidic DMADP (right) pools compared between IE wild-type (black circles) and NE (white circles) leaves of lines RA1 and RA22. Means of $n = 4$ to 8 $\pm$ SE; significance was tested with one-way ANOVA (Tukey's test); $^*P < 0.05$; $^{**}P < 0.01$.

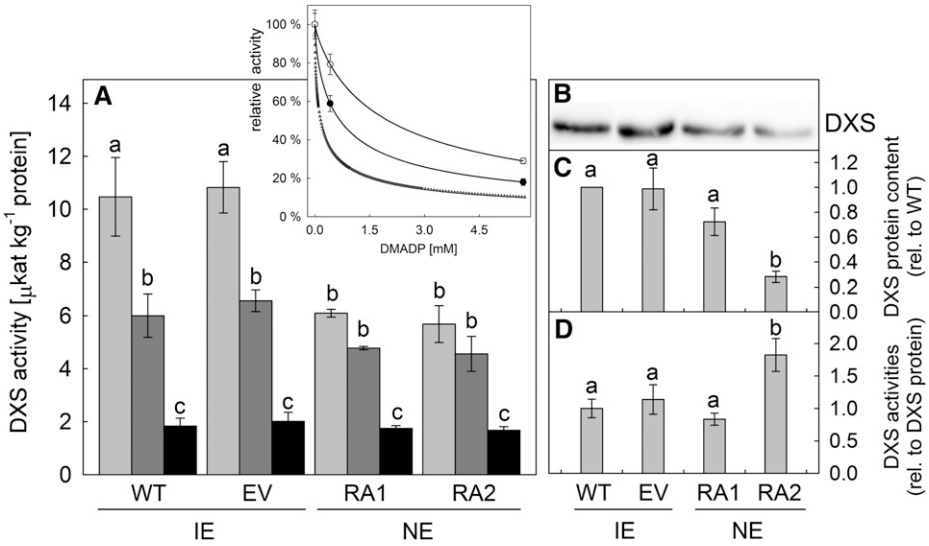

Figure 4. A, In vitro PcDXS activity in the absence (light gray) or presence of low (dark gray) and high (black) DMADP concentrations. Low (0.42 mM) and high (5.7 mM) DMADP represent the in vivo plastidic DMADP concentrations found in IE leaves of the wild type (WT) and EV control from the transformation and NE leaves from the transgenic lines RA1 and RA2, respectively (from ninth leaves from the top, acclimated at 1,000 μmol m^{-2} s^{-1} of incident PPFD, 30°C temperature, and 380 μmol mol^{-1} of CO_2). Representative image of immunoblot analyses of PcDXS protein (67.6 kD) content (B) and quantitative data of PcDXS protein content (C) relative to wild-type plants. D, Relative PcDXS activities normalized per DXS protein content. Means of n = 4 to 5 ± SE are demonstrated. Significance differences (two-way ANOVA followed by Tukey's test) at $P < 0.05$ are indicated with different letters. Inset, Comparison of relative PcDXS activities between IE (wild type and EV; black circles) and NE (RA1 and RA2l; white circles) leaves compared with data obtained on purified DXS protein from *P. trichocarpa* (PtDXS; gray triangles) and assayed at K_m concentration of ThDP (data courtesy of Tom Sharkey and published in Banerjee et al., 2013). The black lines represent the nonlinear curve fitting of experimental data averages in the absence and presence of low and high DMADP concentrations by using Equation 1, where v_{max} was set to 100 and v_{min} to 0. Hill coefficients (H) were 0.61 (PtDXS), 0.72 (IE), and 0.86 (NE); IC_{50} values were 163 (PtDXS), 693 (IE), and 2,005 (NE) μM.

possibility that the plastidic concentration of DMADP feedback inhibits the activity of DXS as postulated by Banerjee et al. (2013). Analysis of apparent PcDXS activity in vitro in the presence of in vivo concentrations of plastidic DMADP measured in IE (0.42 mM) and NE (5.7 mM) leaves adapted to standard conditions (30°C, 1,000 PPFD, 380 [CO_2]) highlighted a concentration-dependent reduction of PcDXS activity independent of the emitter type (Fig. 4A). Incubation of enzyme extracts with the low DMADP concentration of IE plastids reduced PcDXS enzyme activities by 20% and 41% in NE and IE samples, respectively (Fig. 4A, insert). In the presence of high DMADP concentration found in NE plastids, in vitro PcDXS activities were reduced by 70% and 80% in IE and NE enzyme extracts, respectively (insert of Fig. 4A). However, even under the high plastidic DMADP concentration typical for NE plastids, the inhibition of in vitro PcDXS activity was not complete.

The dependency of DXS activity on DMADP concentration could be described by a classical four-parameter logistic curve (insert of Fig. 4A). The resulting Hill coefficients (H) were 0.72 for IE and 0.86 for NE, respectively, i.e. comparable to 0.61 for the purified PtDXS assayed at K_m concentration of thiamin diphosphate (ThDP; Banerjee et al., 2013). The concentrations of DMADP at which relative PcDXS activity became inhibited by half (50% inhibition of initial activity [IC_{50}]) were 693 μM for IE and 2,005 μM for NE, respectively, in contrast to 163 μM for PtDXS. Interestingly, the inhibition of apparent PcDXS activities was less pronounced compared with the inhibition of heterologously expressed *Populus trichocarpa* PtDXS (insert of Fig. 4A, triangles) reported by Banerjee et al. (2013).

In the absence of DMADP, the PcDXS activities in NE were 55% of those from IE extracts, which fairly well coincides with 51% of lower amount of DXS protein content measured by immunoblot analysis (Fig. 4, A–C). The relative PcDXS activities normalized to DXS protein content were not found to be statistically different ($P < 0.05$, ANOVA) between the wild type, empty vector (EV), and RA1 but higher in RA2 (Fig. 4D). Unlike that observed for DXS, the levels of the next enzyme of the pathway, DXR, remained unchanged in NE lines compared with wild-type and EV plants (Supplemental Fig. S2).

To compare the in vivo activities of PcDXS in NE leaves to enzymes from IE leaves, we calculated their activities at the DMADP concentrations occurring in the plastids. PcDXS activities were 6.3 ± 0.4 μkat kg^{-1} protein in IE and 1.7 ± 0.1 μkat kg^{-1} protein in NE leaves, resulting in 27.2% of PcDXS activity in NE

compared with IE leaves. This is very similar to the 28.5% relative PcDXS activity calculated using the kinetics described by Banerjee et al. (2013).

Because IDP also inhibits DXS activity (Banerjee et al., 2013), we aimed to calculate the hypothetical inhibition of PcDXS by taking into account both DMADP and IDP pools using PtDXS kinetics. To achieve this, we compared first the effect of the larger difference in pool sizes between IE and NE when IDP is additionally considered. In NE, the apparent in vitro PcDXS activity due to the sum of DMADP and IDP was calculated to be 23.9% of IE. Similarly, the same difference in pool size between the sum of DMADP and IDP in IE and NE would hypothetically affect the PtDXS activity of 24.9%, based on PtDXS data. Thus, the calculation of hypothetical PcDXS activities based on in vitro enzyme assays from gray poplar leaf protein extracts in the presence of DMADP, as well as calculations based on the enzyme kinetics of heterologously expressed and purified PtDXS (Banerjee et al., 2013), were highly consistent. We therefore finally calculated the theoretical decrease of PcDXS activities between NE and IE by applying PtDXS kinetics and in vivo sum of DMADP and IDP contents and found that NE has at least 13.7% of IE PcDXS activities.

Correlation among MEcDP, Plastidic DMADP, and Isoprene Emission in Emitting Poplars

By plotting metabolite data from illuminated IE plants growing under different temperature, light, and CO_2 conditions, the relationships between MEcDP pool size and isoprene emission (r^2 = 0.89), on the one hand, and MEcDP pool size and plastidic DMADP pool size (r^2 = 0.85), on the other, were determined. These relationships could be described accurately by a two-parameter logistic equation showing that the increase of the MEcDP pool at the low concentration range was directly proportional to the increase of the plastidic DMADP pool and isoprene emission rate, and the relationship saturated at higher MEcDP concentrations (Fig. 5).

Down-Regulation of Carbon Flux through Plastidic Isoprenoid Biosynthesis in NE Poplars

We next calculated the carbon flux through the MEP pathway in IE and NE lines under varying temperature, light, and CO_2 environments. Depending on the environmental condition, the knockdown of *PcISPS* reduced the carbon fluxes into isoprene biosynthesis from 11 to 50 nmol carbon m^{-2} s^{-1} down to 0.2 to 2.3 nmol carbon m^{-2} s^{-1} (Fig. 6, A–C). In terms of percentage, NE plastids exhibited only 0.2% to 3.6% of the isoprene carbon fluxes found in IE.

Generally, the isoprene carbon fluxes are dependent on environmental conditions in a similar way as we observed for plastidic DMADP and MEcDP pools (Fig. 3).

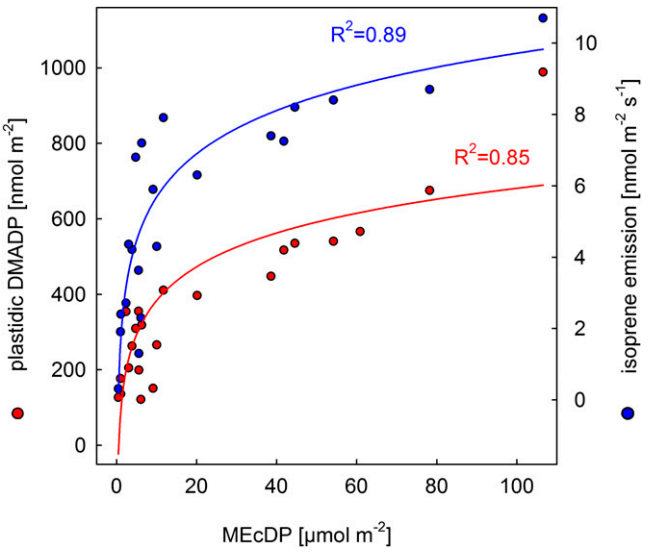

Figure 5. Correlation of MEcDP with calculated plastidic DMADP concentration (red circles) and isoprene emission rate (purple circles) of IE leaves at different leaf temperature (25°C, 30°C, and 35°C), incident PPFD levels (100, 250, 500, and 1,000 μmol m^{-2} s^{-1}), and CO_2 concentration (380, 580, and 780 μmol mol^{-1}). Curves show two-parameter logistic fits (i.e. $y = y_0 + a \ln x$), and the respective coefficients of determination (r^2) are reported next to each fit.

The carbon flux increases with temperature, with a maximum rate at 35°C, followed by a decrease at higher temperature. Increasing light intensities exponentially increased isoprene carbon fluxes, whereas increasing CO_2 concentrations negatively affected these fluxes.

We then focused our attention on the fractions of MEP pathway carbon flux directed toward the biosynthesis of photosynthetic pigments, which represents the other important carbon sink downstream for the products of this pathway. NE leaves showed a significant increase of carbon flux into the biosynthesis of carotenoids and Chls, accompanied by an overall decrease of their absolute content in the leaves (Fig. 7). The ^{13}C analysis of pigments clearly proved that NE leaves demanded more carbon from the MEP pathway to sustain a much faster turnover of β-carotene. Interestingly, the carbon flux into the prenyl side-chain of Chl *a* and *b* became significantly different between IE and NE after an additional 1 h of darkness.

We added up the carbon fluxes going into isoprene and nonvolatile plastidic isoprenoids, assuming that this gives an approximation of the total flux through the MEP pathway in fully mature leaves (Fig. 8). Compiling all data, we could provide evidence that the overall carbon flux through the MEP pathway in NE plastids was strongly reduced compared with the situation in IE plastids (from 26.4 ± 4.7 to less than 1 nmol m^{-2} s^{-1} of carbon equivalent). The partial redirection of the carbon fluxes in NE leaves into nonvolatile isoprenoids from unused carbon for isoprene biosynthesis was very marginal. Only approximately

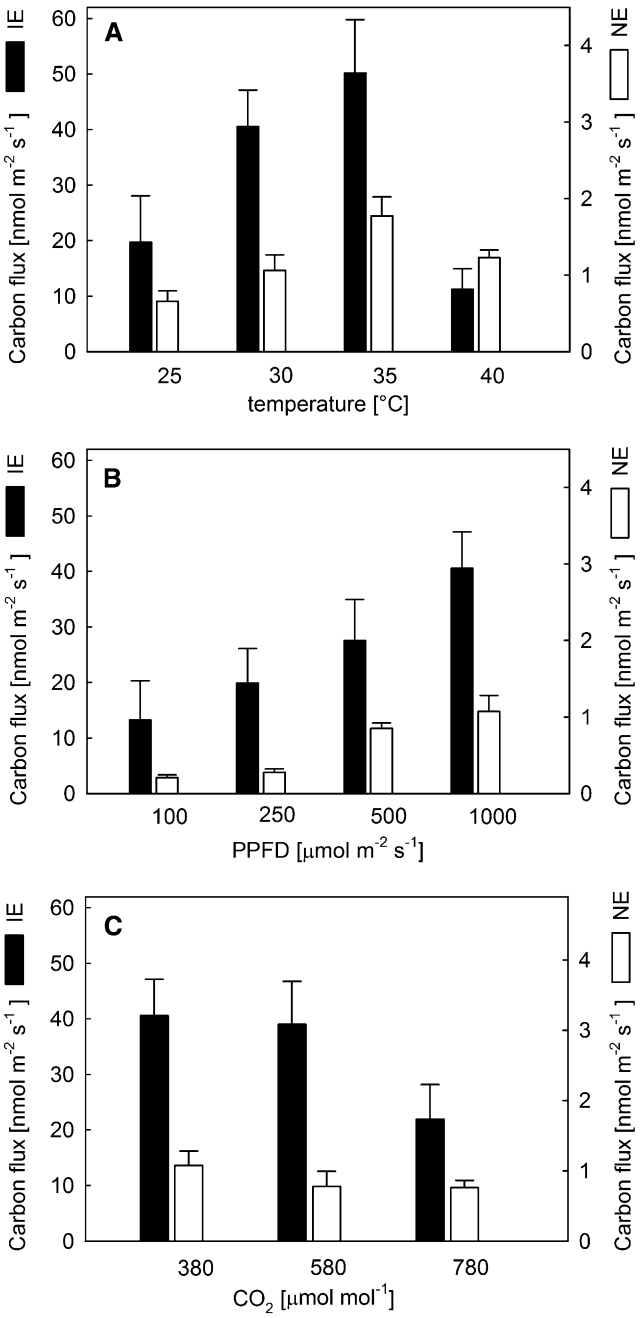

Figure 6. Dependencies of in vivo carbon fluxes through the MEP pathway on temperature (A), light (B), and CO_2 concentration (C) in wild-type IE (black) and NE (white; lines RA22 and RA1) poplar leaves. Note the differences in scale. Means of $n = 4$ (IE) to 8 (NE) ± SE are shown. The fluxes in IE were always significantly different from the fluxes in NE at a level of $P < 0.001$ (one-way ANOVA, Tukey's test).

0.5% of the surplus of carbon was diverted into carotenoid and xanthophyll biosynthesis.

In fully mature IE leaves (leaf number 9 from the top) and under standard conditions (leaf temperature of 30°C, PPFD of 1,000 μmol m^{-2} s^{-1}, [CO_2] of μmol mol^{-1}), almost 99% of carbon directed through the MEP pathway was used for isoprene biosynthesis, and 1% was used for nonvolatile isoprenoid synthesis. Silencing PcISPS resulted in a decrease of overall plastidic carbon demand, although the relatively low isoprene emission of NE leaves still needed a larger fraction of carbon fluxes (54%) than for any other plastidic nonvolatile isoprenoid.

In NE leaves, the plastidic DMADP pool was approximately 20-fold higher than in IE leaves. The higher availability of the C_5 intermediates DMADP and IDP in NE leaves or the need to compensate the lack of isoprene function led to an increased carbon flux into nonvolatile isoprenoids in NE. However, more relevant biochemically, the larger plastidic pool of DMADP and IDP reduced the flux through the MEP pathway due to feedback inhibition of PcDXS.

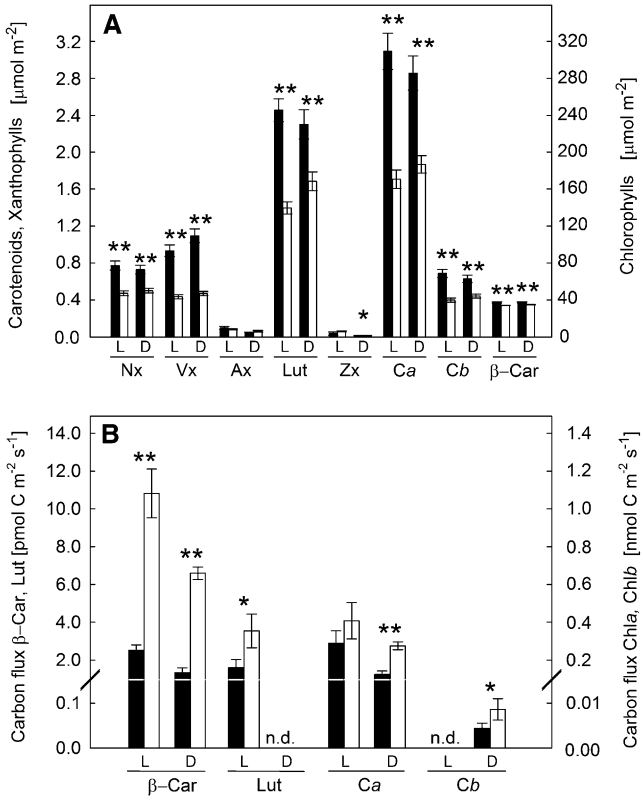

Figure 7. A, Contents of carotenoids, xanthophylls, and Chls contents in the light (L) and followed by 1 h of darkness (D) in wild-type IE (black) and in NE (white; lines RA22 and RA1) poplar leaves (means of $n = 12$ ± SE). B, Calculated carbon fluxes into main carotenoids, xanthophylls, and Chls after $^{13}CO_2$ labeling in the light and followed by 1 h of darkness in wild-type IE (black) and in NE (white; lines RA22 and RA1) poplar leaves (means of $n = 4$ to 8 ± SE). Leaves were acclimated under standard steady-state conditions (incident PPFD of 1,000 μmol m^{-2} s^{-1}, leaf temperature of 30°C, and CO_2 concentration of 380 μmol mol^{-1}). Significance between IE and NE was tested with one-way ANOVA (Tukey's test); $^*P < 0.05$; $^{**}P < 0.01$. β-Car, β-Carotene; Nx, neoxanthin; Vx, violaxanthin; Ax, antheraxanthin; Lut, lutein; Zx, zeaxanthin.

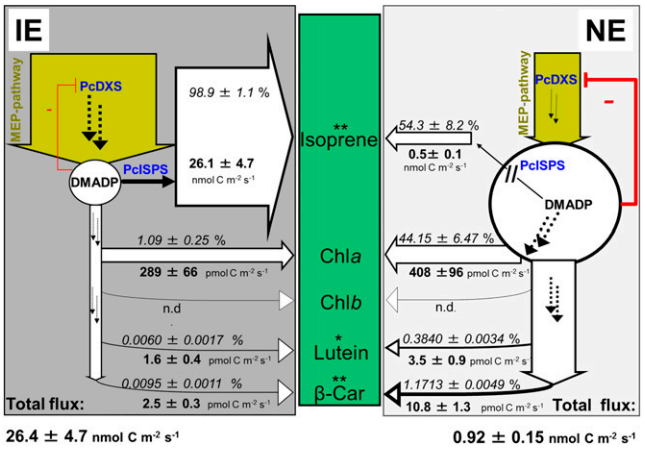

Figure 8. Summary of the carbon fluxes through the MEP pathway into the main products of the plastidic isoprenoid pathway in mature poplar leaves of IE and NE lines under standard steady-state conditions (leaf temperature 30°C, incident PPFD of 1,000 μmol m^{-2} s^{-1}, and CO_2 concentration of 380 μmol mol^{-1}). The demand of carbon from the MEP pathway for each compound is reported as percentage of total carbon flux. β-Car, β-Carotene.

DISCUSSION

MEcDP and Plastidic DMADP Pools Reflect Isoprene Emission under Different Environmental Constraints

^{13}C labeling is a classical approach for studying metabolic fluxes (Rios-Estepa and Lange, 2007) and often used to analyze the dynamics of isoprene (Karl et al., 2002) and monoterpene (Loreto et al., 2000; Ghirardo et al., 2010a) biosynthesis and to dissect the origin of carbon in volatile isoprenoids (Kreuzwieser et al., 2002; Ghirardo et al., 2011; Trowbridge et al., 2012). Here, we applied $^{13}CO_2$ labeling as a tool to measure plastidic DMADP concentrations and to quantify the de novo production of volatile and nonvolatile isoprenoids in IE and NE poplar lines. Importantly, we considered carbon sources other than atmospheric CO_2 for plastidic isoprenoid biosynthesis (Kreuzwieser et al., 2002; Schnitzler et al., 2004; Ghirardo et al., 2011; Trowbridge et al., 2012) to determine the exact carbon flux into nonvolatile isoprenoids by means of maximum ^{13}C-labeling rate into the volatile isoprene, which is continuously produced de novo in the light (Ghirardo et al., 2010a). The concept is proven by obtaining similar carbon fluxes into β-carotene when label was applied as ^{13}C-labeled Glc (^{13}Glc) instead of $^{13}CO_2$ (Supplemental Table S1).

Looking at the ^{13}C-labeling patterns of the isoprenoid metabolites, MEcDP and isoprene were found to be similarly labeled, confirming the close stoichiometric relationship between them. However, the labeling of DMADP was very different, because this intermediate is present in the plastids, cytosol, and mitochondria, and therefore, the rapid incorporation of ^{13}C into plastidic DMADP is diluted by unlabeled DMADP occurring in other cellular compartments. Nevertheless, the amounts of plastidic DMADP can be determined as the postillumination isoprene emission burst (Rasulov et al., 2009a, 2013; Weise et al., 2013) by measuring the isotope ratios of isoprene and total DMADP after short-term labeling with $^{13}CO_2$ (Ghirardo et al., 2010a) or by light-minus-dark measurements (Weise et al., 2013). Assuming that there is negligible exchange of DMADP between the plastid and cytosol within 45 min (Loreto et al., 2004; Wolfertz et al., 2004; Wu et al., 2006), the amount of ^{13}C incorporation into isoprene reflects the ^{13}C incorporated in plastidic DMADP. Comparing the three methods, absolute values of plastidic DMADP estimated by light-minus-dark measurements are found 14% to 15% lower and by postillumination burst 20% higher than the actual reported with the labeling method (data not shown). Absolute amount of nonplastidic DMADP might be found different if light-minus-dark measurements are used (Weise et al., 2013).

Isoprene emission rates depend mainly on the availability of photosynthetic intermediates, the light-dependent delivery of energy, and redox equivalents as well as the amount of ISPS (for review, see Sharkey and Yeh, 2001; Sharkey et al., 2008); all these parameters are similarly affected by environmental constraints (Monson et al., 2012), with the exception of CO_2 concentrations (Rosenstiel et al., 2003; Sun et al., 2012; Way et al., 2013). Changes in light intensity and temperature rapidly affect the pools of MEcDP and plastidic DMADP in IE leaves, which is also reflected in the changes of isoprene emission (Rodríguez-Concepción, 2006; Rasulov et al., 2010; Mongélard et al., 2011). Considering that the ratio of DMADP/IDP is around 2 (Zhou et al., 2013), the concentrations of MEcDP and overall DMADP measured in gray poplar leaves were similar to concentrations measured in hybrid aspen (*Populus tremula* × *Populus alba*) under comparable environmental conditions using a liquid chromatography-tandem mass spectrometry-based analytical approach (Li and Sharkey, 2013b), albeit the authors measured the total sum of both DMADP and IDP pools.

High temperature led to decreased CO_2 assimilation, decreased MEcDP, and plastidic DMADP as well as isoprene emission. Consistently, the MEcDP pool was depleted faster than the DMADP pool when photosynthesis was impaired at 40°C. At high CO_2, which is known to negatively affect isoprene emission (Rosenstiel et al., 2003; Way et al., 2011, 2013), although not at high temperatures (Li and Sharkey, 2013a; Sun et al., 2013a), MEcDP and plastidic DMADP levels were also lower. However, in contrast to the situation in IE poplars, we observed only small changes in the pools of MEcDP and plastidic DMADP in NE plants in response to changing light, temperature, and CO_2. Nevertheless, the weak isoprene emission still present in NE lines responds rapidly to transient heat and light flecks (Behnke et al., 2013), which can be explained by the temperature response of both PcISPS still present in marginal amounts in these plants and by temperature-dependent,

nonenzymatic chemical conversion of DMADP to isoprene under physiological pH (Brüggemann and Schnitzler, 2002b; Ghirardo et al., 2010a).

Allosteric Inhibition of DXS by Plastidic DMADP Regulates the Carbon Flux through the MEP Pathway

Isoprene biosynthesis is the dominant carbon sink in plastidic isoprenoid biosynthesis of mature poplar leaves (Sharkey and Yeh, 2001; Rasulov et al., 2013). Suppression of isoprene biosynthesis by RNA interference led to a drastic overall decrease of carbon flux within the MEP pathway (Fig. 8). Our data indicate a tight control within the plastidic isoprenoid biosynthesis to adjust to the much lower demand for pathway products. We demonstrate that this regulation was almost entirely achieved in vivo in the NE lines by the allosteric inhibition of PcDXS activity in the presence of the high concentrations of plastidic DMADP when PcISPS activity was (almost) absent.

The putative role of DXS in controlling the metabolic flux within the MEP pathway was previously suggested (Lois et al., 2000), based on a strong correlation between carotenoid accumulation and *DXS* transcript levels. This was confirmed with transgenic plants overexpressing *DXS* in Arabidopsis (Estévez et al., 2001), *Solanum lycopersicum* (Enfissi et al., 2005), and *Lavandula latifolia* (Muñoz-Bertomeu et al., 2006). Increased expression of *DXS* (Lange et al., 1998) and other plastidic isoprenoid enzymes (*DXR* and *phytoene synthase*) further supports the importance of the transcriptional regulation in controlling the MEP pathway flux (Mayrhofer et al., 2005), when the demand for photosynthetic pigments increases due to plastid formation and leaf growth. Contrary to these observations, we observed no difference in gene expression of MEP pathway enzymes between IE and NE leaves, although the carbon flux within the MEP pathway differed drastically between them. Knockdown of *PcISPS* affected neither transcript levels of MEP pathway nor cytosolic MVA pathway genes (Supplemental Fig. S1); the latter was tested because IDP and/or DMADP can be slowly exported from the chloroplast to the cytosol and therefore involved in the cross talk of the two pathways (Bick and Lange, 2003; Hemmerlin et al., 2003).

Our comprehensive analysis of gene expression indicates that another regulatory mechanism must exist and prompted us to investigate protein function, in terms of enzyme activity. Previously, we showed that PcDXS activity strongly depends on leaf development, with higher activities in young leaves (Ghirardo et al., 2010b), while correlating well with leaf isoprene emission potential in fully mature leaves. From feeding experiments with dideuterated 1-deoxy-D-xylulose, bypassing the intrinsic 1-deoxy-D-xylulose 5-phosphate biosynthesis in leaves, Wolfertz et al., (2004) proposed a strong in vivo feedback regulation of DXS activity mediated by DMADP and/or other MEP pathway intermediates. Based on this work, Banerjee et al. (2013) demonstrated that DXS activity in vitro is under allosteric control of DMADP and IDP competing with ThDP for the same substrate binding site. Because of these findings, we analyzed the in vitro PcDXS activities in the absence and presence of DMADP. Our results revealed a pronounced reduction of PcDXS activities in the presence of in vivo levels of DMADP. This observation explains to a large extent the decreased carbon flux in the MEP pathway of NE leaves by the inhibition of PcDXS activity in the presence of the very high amounts of plastidic DMADP measured and is completely consistent with the feedback regulation proposed by Wolfertz et al. (2004) and Banerjee et al. (2013). In contrast to the plastidic DMADP pool, the MEcDP pool did not affect the carbon fluxes of isoprenoid biosynthesis (Mongélard et al., 2011). Thus, the central isoprenoid building block of MEP pathway (DMADP) inhibited the PcDXS, the enzyme that catalyzes the first step of this biosynthetic pathway, thus ensuring an adequate carbon flux through the MEP pathway and preventing the synthesis of excess intermediates and isoprenoid precursors. However, our flux and in vitro analyses indicate that regulation based on DMADP supply cannot completely explain the reduced isoprenoid carbon flux in NE leaves (calculated reduction of carbon flux, 86.3%; measured reduction of carbon flux, 96.5%). This points to additional regulatory mechanisms in the MEP pathway.

Emerging evidence suggests that, in addition to the control of gene expression and the enzyme activity, translational, posttranslational, and posttranscriptional regulations are important to modulate the MEP pathway (Guevara-García et al., 2005; Rodríguez-Concepción, 2006; Pulido et al., 2013). Our data showed that the PcDXS protein content was decreased in NE, in a manner similar to the in vitro PcDXS activities, which were approximately 51% and 55% of the levels in IE leaves, respectively. The differences in protein content of PcDXS between the two NE lines RA2 and RA1 coincide with their respective enzyme activities previously seen (Ghirardo et al., 2010b). Together, our data suggest: (1) a posttranscriptional control of PcDXS protein levels (but not of PcDXR; Supplemental Fig. S2) and (2) that posttranslational modification of PcDXS plays a minor role in the regulation of PcDXS activities because the lower enzyme activities reflected the decreased protein content in NE leaves. The similarities between transcript levels of DXS in IE and NE plants, together with a reduction of both DXS amounts and DXS activities in NE plants, suggest that either differences in the efficiency of translation or protein turnover during protein quality control is involved (Pulido et al., 2013).

Our experiments were restricted to the main isoprenoid compounds (isoprene and photosynthetic pigments) and did not take into account the production and turnover of other putative minor metabolic sinks branching off from the MEP pathway. Although

likely biosynthesized at low rates in poplar leaves, biosynthesis of gibberellins and abscisic acid (derived from zeaxanthin); monoterpenes (no detectable emission in this case); iridoids (monoterpene glycosides); tocopherols, plastoquinone, and, in general, prenylated compounds (proteins and other compounds; Gerber et al., 2009); and export of IDP into the cytosol (Bick and Lange, 2003; Laule et al., 2003) may significantly contribute to the real carbon flux through the MEP pathway.

In support of this assumption are recent metabolomic data that revealed a relatively higher abundance of iridoids in NE than in IE (Way et al., 2013), although carbon fluxes and absolute abundance of these monoterpene glycosides have not been investigated in poplar leaves so far. Cross talk between the MEP and MVA pathways could also represent a sink for MEP pathway products. Evidence for such cross talk comes from experiments using inhibitors of the respective pathways (Kasahara et al., 2002; Hemmerlin et al., 2003; Laule et al., 2003). In snapdragon (*Antirrhinum majus*) flowers, the cross talk seems to occur unidirectionally from the plastids to the cytosol at the level of IDP (Dudareva et al., 2005). Another sink is the diversion of MEcDP from the pathway that acts as a retrograde signal, influencing the expression of targeted stress-responsive genes in Arabidopsis nuclei under stress (Xiao et al., 2012). Transgenic Arabidopsis plants overexpressing *DXS* were also shown to export MEcDP to compensate for the increased flux into the MEP pathway (L.P. Wright, J.M. Rohwer, A. Ghirardo, A. Hammerbacher, M. Ortiz, B. Raguschke, J.-P. Schnitzler, J. Gershenzon, and M.A. Phillips, unpublished data). However, in all studies published so far, the exchange of intermediates and products between the MVA and MEP pathways and diversion of MEcDP appear to be slow processes. Therefore, the transport of isoprenoid intermediates across the plastid envelope seems to be very limited within our 45 min of ^{13}C labeling.

Absence of Isoprene Enforces Higher Turnover of Essential Isoprenoids

The general down-regulation of carbon flux toward the C_5 intermediates DMADP and IDP in NE occurs concurrently with increasing carbon fluxes toward the C_{40} isoprenoids β-carotene and lutein. Considering the amount of carbon needed for isoprene biosynthesis, NE leaves redirected approximately 0.5% of this saved carbon toward essential isoprenoids. This observation coincides with an increased level of monoterpene glycosides (iridoids; Way et al., 2013) in these genotypes.

The relatively low amount of carbon reinvested into essential nonvolatile isoprenoids may simply reflect the low need for nonvolatile isoprenoids in fully mature leaves under unstressed conditions. Considering the net CO_2 assimilation rate as base, the fully mature poplar leaf number 9 invested 0.01% of photosynthetic carbon into pigment biosynthesis and 2.6% in isoprene emission, similar to previously reported values of 0.02% and 2%, respectively (Sharkey and Yeh, 2001). However, stress conditions could significantly change the fluxes in mature leaves if rapid synthesis of essential isoprenoids is needed for repairing the photosynthetic apparatus (Cazzonelli and Pogson, 2010).

The metabolic situation in young, developing poplar leaves is different, and such leaves divert most of their carbon flux into essential isoprenoid biosynthesis, rather than into isoprene emission (Rasulov et al., 2013). This coincides with the developmental activation of MEP pathway genes and DXS activity already discussed above (Guevara-García et al., 2005; Loivamäki et al., 2007; Ghirardo et al., 2010b). Here, redirection of flux from isoprene might be expected to lead to much more substantial investment in nonvolatile isoprenoids, but isoprene formation rates are much lower in young leaves, so there is much less flux to redirect.

The enhanced carbon flux toward essential isoprenoids in NE leaves compared with IE leaves might simply be a consequence of the increased availability of plastidic DMADP because biosynthesis of carotenoids and the phytol side-chain of Chl compete for the same DMADP pool as isoprene (Rasulov et al., 2013). However, the higher carotenoid and Chl content as seen here and in previous studies (Behnke et al., 2007; Way et al., 2013) might be mediated by the higher turnover of essential isoprenoids due to the absence of isoprene emission. Because both isoprene (Loreto and Velikova, 2001; Peñuelas et al., 2005; Vickers et al., 2009; Loreto and Schnitzler, 2010) and carotenoids (Cazzonelli and Pogson, 2010) play crucial roles as antioxidant agents in leaves, the absence of isoprene might be counterbalanced by increases in the higher molecular weight carotenoids (Behnke et al., 2007; Way et al., 2011, 2013; Behnke et al., 2013). Evidence of these metabolic changes is also revealed by the remodeling of the plastid proteome (Velikova et al., 2014).

The fact that NE plants do not redirect all the carbon saved from isoprene production to the formation of photosynthetic pigments appears to benefit them in other ways by making more fixed carbon and energy available for general metabolic purposes. Recent studies on gray poplar (Behnke et al., 2012) and tobacco (*Nicotiana tabacum*; Ryan et al., 2014) demonstrate that lower isoprene emission is accompanied by greater biomass production.

CONCLUSION

Isoprene biosynthesis in mature poplar leaves is by far the main carbon sink of MEP pathway intermediates, and its production requires several-fold higher carbon fluxes than in NE plants. Thus, removal of the capability to emit isoprene by RNA interference of isoprene synthase drastically diminished the overall carbon fluxes within the MEP pathway because only a small portion of unused isoprene intermediates were channeled downstream toward the biosynthesis of

carotenoids and Chls. These may have helped compensate for changes in plastid functionality and the overall performance of the photosynthetic apparatus in the absence of isoprene. Under these conditions, flux regulation in the MEP pathway is mediated by feedback control of plastid DMADP levels on the in vivo activity of DXS. With its high isoprene emission capacity and concurrent high metabolic fluxes through the MEP pathway, poplar represents an ideal system for studying the regulation of this central biosynthetic pathway in plants.

MATERIALS AND METHODS

Plant Material and Experimental Set-Up

We investigated the metabolic carbon fluxes through the MEP pathway using IE wild-type and EV as control plants (for the transgenic manipulation) as well as transgenic NE plants (lines RA1 and RA22; for more details on the plant lines, see Behnke et al., 2007) of 3-year-old gray poplar (*Populus* × *canescens*) trees. In the transgenic lines, the isoprene synthase expression was silenced by an RNA interference technique, resulting in plants with very low isoprene emission capacity (Behnke et al., 2007, 2010b, 2013). Cultivation and growth conditions were as previously described (Behnke et al., 2007; Cinege et al., 2009).

Fully mature leaves, from the eighth or ninth node from the apical meristem were detached, and the petiole were placed in a 2-mL vial filled with 10 mM unlabeled Glc (^{12}Glc) dissolved in autoclaved Long Ashton nutrient solution (Ehlting et al., 2007). Each leaf was then enclosed in a gas exchange cuvette, and VOC measurements were performed using the system described previously (Ghirardo et al., 2011). The cuvettes were flushed with humidified (relative humidity of 60%), synthetic VOC-free air (380 μmol mol^{-1} CO_2, 21.0% [v/v] O_2 in N_2; BASI Schöberl) at a flow rate of 1 L min^{-1}. We conducted steady-state experiments under standard conditions, consisting of PPFD of 1,000 μmol m^{-2} s^{-1}, leaf temperature of 30°C, and atmospheric CO_2 concentration of 380 μmol mol^{-1}. Before applying the ^{13}C label, leaves were always acclimated for 1 h in the cuvettes to ensure that gas exchange of water and CO_2 and isoprene emissions had reached the steady-state conditions.

The ^{13}C label was applied for 45 min either by replacing the unlabeled CO_2 with $^{13}CO_2$ (380 μmol mol^{-1}; 99 atom % [w/w] ^{13}C; Air Liquide) or by changing the unlabeled Glc solution with an equimolar fully ^{13}C-labeled ^{13}Glc solution (99 atom % [w/w] ^{13}C; Cambridge Isotope Laboratories) without exposing the leaves to the air. For each labeling experiment, we performed the corresponding control experiment using unlabeled substrate.

We investigated the effect of photosynthesis on the pool of MEP pathway metabolites by comparing leaves fed for 45 min under light condition with leaves labeled additionally for 1 h in darkness. At the end of the experiment, leaves were sampled by flash freezing under liquid N_2 and stored at –80°C for further analysis.

In similar experiments, we used leaves from intact plants to investigate the effect of different environmental conditions on the MEP pathway. For this purpose, light (PPFD = 100, 250, 500, and 1,000 μmol m^{-2} s^{-1}), temperature (25°C, 30°C, 35°C, and 40°C), or CO_2 concentration (380, 580, and 780 μmol mol^{-1}) differed from the standard conditions.

For testing the PcDXS activities and measuring the gene expression, 20 additional plants (five plants of each line wild type, EV, RA1, and RA2) were acclimated for 2 d into a phytotron chamber at the Research Unit Environmental Simulation (Helmholtz Zentrum München) under the ambient climate conditions of 26°C/18°C (day/night), relative humidity of 60%/80% (day/night), PPFD of 500 μmol photons m^{-2} s^{-1} for a 16-h photoperiod, and CO_2 concentration of 380 μmol mol^{-1}. The ninth leaves from apices were sampled at 12 AM (Central European Time) after changing the environmental conditions to 30°C and 1,000 μmol m^{-2} s^{-1} for 1 h.

Quantification and Isotopic ^{13}C Compositions of MEcDP, DMADP, and Isoprene

Absolute quantification and isotopic composition analysis of isoprene and its immediate precursor DMADP was performed using proton transfer reaction mass spectrometry by measuring the protonated isotopologue masses as described previously (Ghirardo et al., 2010a, 2011). We measured DMADP as isoprene released after acid hydrolysis as described by Brüggemann and Schnitzler (2002b). Plastidic DMADP was calculated from the amount of ^{13}C incorporated into the total DMADP pool and isoprene as described previously (Ghirardo et al., 2010a). In brief, under steady-state conditions and short exposure times of leaves to $^{13}CO_2$, the isotopic pattern of isoprene reflects the isotopic pattern of the plastidic DMADP. Thus, the proportion of plastidic and nonplastidic DMADP pools can be derived from measuring the total DMADP pool and the ^{13}C-labeling patterns of total DMADP (plastidic and nonplastidic) and naturally emitted isoprene.

For MEcDP analyses, 5 mg of lyophilized plant material was extracted twice with a 250-μL solution of 50% acetonitrile containing 10 mM ammonium acetate by vortexing for 5 min, centrifuging for 5 min at 16,000*g*, and then transferring 200 μL of each supernatant to a new tube (Eppendorf). The combined extracts (400 μL in total) were dried under N_2 at 40°C, and the residue was dissolved in 100 μL of 10 mM ammonium acetate and transferred to a new tube. After extracting the solution with 100 μL of chloroform and phase separation through centrifugation at 16,000*g* for 5 min, the upper aqueous phase was transferred to a new tube and diluted with the same volume of acetonitrile. After centrifugation for 5 min at 16,000*g*, the supernatant was transferred to an HPLC vial. The MEcDP and its ^{13}C incorporation were analyzed on an Agilent 1200 HPLC system connected to an API 3200 triple quadrupole mass spectrometer (MS). For separation, an Atlantis HILIC column (3 μm, 150 × 2.1 mm; Waters) with a SecurityGuard HILIC guard column (4 × 3 mm; Phenomenex) and a KrudKatcher high-pressure precolumn filter (Phenomenex) were used. The solvents used were 10 mM ammonium acetate in pure water (purity > 18 MΩ at 25°C) as solvent A and acetonitrile:water (9:1, v/v) containing 10 mM ammonium acetate as solvent B. Separation was achieved with a flow rate of 500 μL min^{-1} and a column temperature of 40°C. The solvent gradient profile was: 10-min linear gradient from 0% to 30% of solvent A, 5-min wash step at 40% with solvent A, 0.1 min for returning to initial conditions, and 4.9 min for further equilibration. The volume injected was 10 μL. The MS was used in negative ionization mode with the following instrument settings: ion spray voltage, 4,500 eV; turbo gas temperature, 700°C; nebulizer gas pressure, 483 kPa; heating gas pressure, 207 kPa; curtain gas pressure, 207 kPa; and collision gas pressure, 60 kPa. MEcDP and its isotope distribution was monitored as analyte precursor ion → quantifier ion: mass-to-charge ratio (m/z) 276.7 → 78.8, m/z 277.7 → 78.8, m/z 278.7 → 78.8, m/z 279.7 → 78.8, m/z 280.7→ 78.8, and m/z 281.7 → 78.8 for MEcDP containing 0, 1, 2, 3, 4, or 5 ^{13}C, respectively. The quantifier ion used was phosphate, which does not contain any carbon atoms and can thus be monitored as the same mass for the different labeled molecules. The settings of the instrument were: collision energy, –54 V; declustering potential, –40 V; cell entrance potential, –30 V; cell exit potential, –0 V; and entrance potential, –8 V. Both Q1 and Q2 quadrupoles were maintained at high mass resolution of approximately 0.5 D. Analyst 1.5 software (Applied Biosystems) was used for data acquisition and processing. The MEcDP content in the plant extracts were quantified using external standard curves and normalized to additionally added (3,4,5-^{13}C)-MEcDP internal standard (ISTD; Illarionova et al., 2006). Normalization to added labeled standards was accomplished by analyzing each plant sample twice, once without any added ISTD and the second time with the addition of MEcDP ISTD dissolved in 10 μL water. The ISTD solution was added directly after adding the first extraction solvent to the dried plant material. Labeled samples consisted of ions with m/z values ranging from m/z 276.7 up to m/z 281.7. The MEcDP ISTD, containing (3,4,5-^{13}C)-MEcDP isotopic label, has m/z 279.7. The amounts of the other mass peaks of the sample with added ISTD can be used to determine the amount of m/z 279.7 originating from the plant material, when compared to the values obtained for the sample not containing any added ISTD. In this way, the signal originating from the added ISTD and that from the plant material can be determined, thereby using the added MEcDP as ISTD to quantify the absolute quantities of MEcDP. In this way, any matrix effect during the extraction as well as any ion suppression effects in the MS could be accounted for.

RNA Extraction, Reverse Transcription PCR, and Real-Time PCR

Total RNA was extracted from 50 mg frozen leaf material using the Plant RNeasy extraction kit (Qiagen) and following manufacturer's instructions. The RNA concentration was accurately quantified by spectrophotometer measurements using a NanoDrop 1000 photometer, (Peqlab GmbH), and complementary DNAs were synthesized by Omniscript RT Kit (Qiagen) using 1 μg RNA.

The primers for the selected genes of the MEP pathway, i.e. 1-deoxy-D-xylulose-5-phosphate synthase (*PcDXS*), 1-deoxy-D-xylulose-5-reductoisomerase (*PcDXR1*, *PcDXR2*), diphosphocytidyl methylerythritol kinase (*PcCMK*), and 4-hydroxy-3-methylbut-2-en-1-yl diphosphate reductase (*PcHDR*), and of the MVA pathway, i.e. 3-hydroxy-3-methylglutaryl coenzyme (*PcHMGR*) and MVA kinase (*PcMEV*), were designed and tested for their specificity (for the primer sequences, see Supplemental Table S2). The primers for the genes *DXR1* and *CMK* are as in Wiberley et al. (2009).

Real-time PCR was performed on a 7500 Fast Real-Time PCR system (Applied Biosystems) using the SensiFAST SYBR Lo-ROX kit (Bioline). Five biological replicates for each plant line (IE: lines wild type and EV; NE: lines RA1 and RA2) were assayed, each with three technical replicates. The reference gene Actin2 was included in each plate.

PCR was carried out in a volume of 20 μL, with 2× SensiFAST SYBR Lo-ROX 10 μL, 10 μM forward/reverse primers, and 1 μL and 5 μL complementary DNA templates, respectively. PCR conditions were as follows: 1 cycle at 95°C for 2 min, 40 cycles at 95°C for 15 s, 60°C for 30 s, and a dissociation stage including two cycles at 95°C for 15 s and 60°C for 1 min. Samples were subjected to autocycle threshold for analysis, and dissociation curves were verified for each gene.

Determination of in Vitro PcDXS Activity and Immunoblot Analysis

The measurement of PcDXS enzyme activities from plant leaves were determined under V_{max} conditions to get a quantitative value for the amount of active PcDXS enzyme in different plant lines. Fresh plant tissue was homogenized under liquid nitrogen, and approximately 20 mg was extracted and assayed for DXS activity as described (Pulido et al., 2013). Enzyme activity was then normalized to protein content as determined by the Bradford assay. To measure the possibility of feedback inhibition of DXS by DMADP, the PcDXS activity was also determined in the presence of DMADP (Sigma-Aldrich) at concentrations that occur in vivo in IE (0.42 mM) and NE (5.7 mM) plants. After the enzyme reaction was stopped, the 1-deoxy-D-xylulose 5-phosphate produced was measured on the same HPLC-MS system used for MEcDP analysis with the different set-up: an XBridge Amide column (3.5 μm, 150 × 2.1 mm, Waters) with a HILIC guard column containing the same sorbent (3.5 μm, 10 × 2.1 mm) was used. The solvents used were 20 mM ammonium bicarbonate adjusted to pH 10.0 with ammonium hydroxide (25% [v/v]) as solvent A and acetonitrile:water (80:20, v/v) containing 20 mM ammonium bicarbonate (pH 10.0) as solvent B. Separation was achieved with a flow rate of 500 μL min^{-1} and a column temperature of 25°C. The solvent gradient was as follows: 5-min linear gradient from 0% to 16% with solvent A, 5-min isocratic separation, 5 min with 40% solvent A, a return to 0% solvent A over 0.1 min, and 4.9 min for further equilibration. The volume injected was 1 μL. The MS was run in the same way as for MEcDP analysis with the following modifications: analyte precursor ion → quantifier ion scan combinations, m/z 212.95→138.9 and m/z 215.95 → 140.9 (collision energy, –18 V; declustering potential, –60 V; and cell exit potential, –15 V).

The protein content of PcDXS was quantified by immunoblot analysis as described previously (Pulido et al., 2013). As control, PcDXR protein levels were quantified in parallel.

Inhibitory Effect of Plastidic DMADP/IDP on PcDXS Activities and Consequences for Isoprene Emission

The in vivo inhibitory effect of DMADP and IDP on DXS activity was calculated following Banerjee et al. (2013) by using the four-parameter logistic curve equation:

$$v = v_{min} + \frac{v_{max} - v_{min}}{1 + \left(\frac{[I]}{IC_{50}}\right)^{H}} \quad (1)$$

where v was the percentage of DXS activity, v_{min} and v_{max} were set to 0 and 100, respectively, and I was either plastidic DMADP or IDP concentrations (in μM). H was 0.61 ± 0.06 for DMADP and 0.69 ± 0.03 for IDP. The concentration of the inhibitors at which the PtDXS activity was reduced by one-half (IC_{50}) was 163 ± 21 μM for DMADP and 131 ± 9 μM for IDP. IC_{50} and H values were kindly provided by Tom Sharkey from data published in Banerjee et al. (2013) and measured at K_m of ThDP on PtDXS cloned from *Populus trichocarpa* heterologously expressed and purified from *Escherichia coli*. For comparison, we aimed to assess the hypothetical PcDXS activities based on the enzyme kinetics of PtDXS. The inhibition of PcDXS was simulated taking both DMADP and IDP pools as a sum, using the in vivo occurring plastidic DMADP concentration of 0.42 mM for IE and 5.7 mM for NE and assuming that the ratio of DMADP/IDP was 2.11 (Zhou et al., 2013).

Plastidic concentrations of DMADP were calculated using 23 chloroplasts per palisade mesophyll cell and 12 chloroplasts per spongy mesophyll cell and a chloroplast volume of 15 μm^3 for both cell tissues (Ivanova et al., 2009). Numbers of cells were counted from images of leaf cross sections taken with a confocal scanning laser microscope (Zeiss LSM 510 upright confocal with LSM IMAGE BROWSER software) over an area of 10,000 μm^2. The mean of total cell numbers in one palisade (53 ± 2.5) and spongy (26 ± 4) mesophyll layer was multiplied by the numbers of palisade (two) and spongy (three) mesophyll layers observed in each leaf cross section (n = 4).

Photosynthetic Pigment Contents and Carbon Flux Calculation

Pigments were extracted and quantified by HPLC as described previously (Behnke et al., 2007). Qualitative pigment analysis of $^{13/12}$C was performed combining thin-layer chromatography with IRMS, which allowed the detection of very low changes in the ^{13}C signature ($^{13}C/^{12}C > 1.3 \times 10^{-6}$, i.e. measurement errors of ±0.1% δ^{13}C, relative to Vienna Pee Dee Belemnite). First, 200 μL of the pigment extract used for HPLC analysis was loaded into a carbon-free, silica glass gel thin-layer chromatography plate (Merck) and developed for 1 h with petroleum-benzin:isopropanol:water (100:12:0.2, v/v/v). After the run, four spots were identified as Chl *a*, Chl *b*, β-carotene, and lutein (neoxanthin, violaxanthin, zeaxanthin, and antheraxanthin were neglected due to their very low abundance) by comparing bands of purified pigments derived from flash chromatography (Behnke et al., 2007). These spots were scraped, collected, and freeze dried. Then, 1 mg of the spot was transferred into a tin capsule (HEKAtech GmbH) and flash combusted in an elemental analyzer (Flash EA 1112, Carlo Erba Instruments) equipped with a gas chromatography column (Porapack QS 50/80 mesh, Waters) and coupled to an IRMS (DeltaPlusXP, Thermo Fisher Scientific). The instrument was calibrated according to Werner and Brand (2001) and Coplen et al. (2006) using three primary standards (IAEA C6, Suc; USGS40, L-Glu; and USGS41, L-Glu) purchased directly from the International Atomic Energy Agency, and routine calibration checks were conducted every 11 samples with secondary standard urea (Sigma Aldrich) every 11 samples.

The ^{13}C fluxes from the ^{13}C-labeling source to the photosynthetic pigments were calculated as follows:

$$^{13}C_{flux} = \frac{\left(^{13}Cs - ^{13}Cc\right) P\, Cn}{\Delta t\, D} \quad (2)$$

where $^{13}C_s$ and $^{13}C_c$ are the amounts of ^{13}C at the end of experiment with labeled sample and unlabeled control, respectively; P is the amount of pigment (in nmol), Δt is the labeling time (s), D is the dry weight of the sample (in mg), and C_n is the number of C atoms that formed the isoprenoid part of the pigment (20 carbon atoms for the prenyl side-chains of Chls and 40 for the carotenoids β-carotene and lutein). The incorporation of ^{13}C into the pigments was finally used to calculate the real carbon flux into the pigments. Because some unlabeled carbon is also normally used in de novo biosynthesis of plastidic isoprenoid during $^{13}CO_2$ labeling (Ghirardo et al., 2011), the ^{13}C data only represent the apparent carbon flux. To calculate the real carbon flux into pigment biosynthesis, the apparent carbon flux was multiplied by 100 and divided by the percentage of labeled isoprene during steady state, thus taking into account the unlabeled ^{12}C that was unavoidably incorporated in the de novo biosynthesis of the isoprenoid (Ghirardo et al., 2010a).

To be comparable with other emission data, the fluxes normalized with respect to dry weight were related to unit leaf area by multiplying with leaf dry mass per unit area (63.7 g dry weight m^{-2}; n = 32).

Determination of Carbon Fluxes into Isoprene Biosynthesis through the MEP Pathway

Fluxes of carbon into isoprene biosynthesis were determined in vivo by measuring the incorporation rate of ^{13}C into isoprene biosynthesis with proton transfer reaction mass spectrometry after $^{13}CO_2$ labeling.

The incorporation rates of ^{13}C into isoprene were normalized relative to 100%, and the experimental data points were fit with the three-parameter Hill equation:

$$f(x) = ax^b \left(c^b + x^b\right)^{-1} \quad (3)$$

where a, b, and c are the empirical parameters, representing the maximum asymptote, the slope factor, and the inflection point of the curve, respectively.

Because the atmospheric CO_2 is not the only carbon source of isoprene biosynthesis (Kreuzwieser et al., 2002; Affek and Yakir, 2003; Schnitzler et al., 2004; Brilli et al., 2007; Ghirardo et al., 2011; Trowbridge et al., 2012), we corrected the fitted parameters for the conditions where the labeling rate (and, hence, the parameter a) represents 100% ^{13}C incorporation. In this case, the parameters of Equation 2 were adjusted as follows: $a_1 = 1$, $b_1 = b$, and $c_1 = ac$. With these parameters, the derivative of the Equation 3 was:

$$f'(x_1) = \frac{\left(a_1 b_1 x^{(b_1-1)}\right)}{\left(x^{b_1} + c_1^{b_1}\right)} - \frac{\left(a_1 b_1 x^{(2b_1-1)}\right)}{\left(x^{b_1} + c_1^{b_1}\right)^2} \quad (4)$$

Equation 4 gives the slope at the inflection point of the incorporation rate of ^{13}C into isoprene, with x_1 being the value at the inflection point, so that $x_1 = c$. To obtain the carbon flux into isoprene biosynthesis, the solution of Equation 4 was multiplied by the isoprene emission rate (in nmol m^{-2}). Fluxes are presented as total carbon by multiplying the number of carbon atoms of isoprene (i.e. 5). All the measurements were performed under steady-state environmental conditions with net assimilation and isoprene emission constant, i.e. when the DMADP content did not change significantly.

Calculation of the Overall ^{13}C Fluxes through the MEP Pathway

The apparent overall carbon fluxes through the MEP pathway were estimated by adding up all separately measured carbon fluxes to the nonvolatile isoprenoids β-carotene, lutein, the prenyl side-chains of Chl *a* and *b*, and the carbon fluxes into isoprene biosynthesis. As monoterpene emission was below the detection limit, it was neglected. The carbon flux of each compound was finally related to the overall carbon flux of the MEP pathway and expressed on a percentage basis.

Statistical Analysis

The statistical significance of differences between IE and NE was tested with one- and two-way ANOVAs and post hoc Tukey's tests. The statistical analysis and curve fitting were performed with Sigma-Plot 11.0 (Systat Software).

Supplemental Data

The following materials are available in the online version of this article.

Supplemental Figure S1. Transcript levels of the genes on methylerythritol 4-phosphate (MEP)-pathway (*PcDXS, PcDXR1, PcDXR2, PcCMK, PcHDR*) and mevalonate pathway (*PcHMGR, PcMEV*).

Supplemental Figure S2. Immunoblot analyses of PcDXR protein content.

Supplemental Table S1. Comparison of carbon fluxes into the biosynthesis of β-carotene after $^{13}CO_2$ or ^{13}Glc feeding.

Supplemental Table S2. Primer sequences, annealing temperatures, and the amplicon lengths in the real-time PCR analysis of mRNA transcript levels.

ACKNOWLEDGMENTS

We thank Rudolf Maier for help during IRMS analysis and Felix Rohdich, Adelbert Bacher, and Wolfgang Eisenreich for the kind gift of ^{13}C-labeled MEcDP.

Received January 17, 2014; accepted March 3, 2014; published March 3, 2014.

LITERATURE CITED

Affek HP, Yakir D (2003) Natural abundance carbon isotope composition of isoprene reflects incomplete coupling between isoprene synthesis and photosynthetic carbon flow. Plant Physiol **131:** 1727–1736

Archibald AT, Levine JG, Abraham NL, Cooke MC, Edwards PM, Heard DE, Jenkin ME, Karunaharan A, et al (2011) Impacts of HO_x regeneration and recycling in the oxidation of isoprene: consequences for the composition of past, present and future atmospheres. Geophys Res Lett **38:** L05804, DOI: 10.1029/2010GL046520

Arneth A, Monson RK, Schurgers G, Niinemets Ü, Palmer PI (2008) Why are estimates of global terrestrial isoprene emissions so similar (and why is this not so for monoterpenes)? Atmos Chem Phys **8:** 4605–4620

Banerjee A, Wu Y, Banerjee R, Li Y, Yan H, Sharkey TD (2013) Feedback inhibition of deoxy-D-xylulose-5-phosphate synthase regulates the methylerythritol 4-phosphate pathway. J Biol Chem **288:** 16926–16936

Behnke K, Ehlting B, Teuber M, Bauerfeind M, Louis S, Hänsch R, Polle A, Bohlmann J, Schnitzler JP (2007) Transgenic, non-isoprene emitting poplars don't like it hot. Plant J **51:** 485–499

Behnke K, Ghirardo A, Janz D, Kanawati B, Esperschütz J, Zimmer I, Schmitt-Kopplin P, Niinemets Ü, Polle A, Schnitzler JP, et al (2013) Isoprene function in two contrasting poplars under salt and sunflecks. Tree Physiol **33:** 562–578

Behnke K, Grote R, Brüggemann N, Zimmer I, Zhou G, Elobeid M, Janz D, Polle A, Schnitzler JP (2012) Isoprene emission-free poplars: a chance to reduce the impact from poplar plantations on the atmosphere. New Phytol **194:** 70–82

Behnke K, Kaiser A, Zimmer I, Brüggemann N, Janz D, Polle A, Hampp R, Hänsch R, Popko J, Schmitt-Kopplin P, et al (2010a) RNAi-mediated suppression of isoprene emission in poplar transiently impacts phenolic metabolism under high temperature and high light intensities: a transcriptomic and metabolomic analysis. Plant Mol Biol **74:** 61–75

Behnke K, Kleist E, Uerlings R, Wildt J, Rennenberg H, Schnitzler JP (2009) RNAi-mediated suppression of isoprene biosynthesis in hybrid poplar impacts ozone tolerance. Tree Physiol **29:** 725–736

Behnke K, Loivamäki M, Zimmer I, Rennenberg H, Schnitzler JP, Louis S (2010b) Isoprene emission protects photosynthesis in sunfleck exposed grey poplar. Photosynth Res **104:** 5–17

Beisel KG, Jahnke S, Hofmann D, Köppchen S, Schurr U, Matsubara S (2010) Continuous turnover of carotenes and chlorophyll a in mature leaves of Arabidopsis revealed by $^{14}CO_2$ pulse-chase labeling. Plant Physiol **152:** 2188–2199

Bick JA, Lange BM (2003) Metabolic cross talk between cytosolic and plastidial pathways of isoprenoid biosynthesis: unidirectional transport of intermediates across the chloroplast envelope membrane. Arch Biochem Biophys **415:** 146–154

Brilli F, Barta C, Fortunati A, Lerdau M, Loreto F, Centritto M (2007) Response of isoprene emission and carbon metabolism to drought in white poplar (*Populus alba*) saplings. New Phytol **175:** 244–254

Brüggemann N, Schnitzler JP (2002a) Relationship of isopentenyl diphosphate (IDP) isomerase activity to isoprene emission of oak leaves. Tree Physiol **22:** 1011–1018

Brüggemann N, Schnitzler JP (2002b) Diurnal variation of dimethylallyl diphosphate concentrations in oak (*Quercus robur*) leaves. Physiol Plant **115:** 190–196

Cazzonelli CI, Pogson BJ (2010) Source to sink: regulation of carotenoid biosynthesis in plants. Trends Plant Sci **15:** 266–274

Chang MCY, Keasling JD (2006) Production of isoprenoid pharmaceuticals by engineered microbes. Nat Chem Biol **2:** 674–681

Cinege G, Louis S, Hänsch R, Schnitzler JP (2009) Regulation of isoprene synthase promoter by environmental and internal factors. Plant Mol Biol **69:** 593–604

Coplen TB, Brand WA, Gehre M, Gröning M, Meijer HAJ, Toman B, Verkouteren RM (2006) New guidelines for $\delta^{13}C$ measurements. Anal Chem **78:** 2439–2441

Delwiche CF, Sharkey TD (1993) Rapid appearance of ^{13}C in biogenic isoprene when $^{13}CO_2$ is fed to intact leaves. Plant Cell Environ **650:** 587–591

Dudareva N, Andersson S, Orlova I, Gatto N, Reichelt M, Rhodes D, Boland W, Gershenzon J (2005) The nonmevalonate pathway supports both monoterpene and sesquiterpene formation in snapdragon flowers. Proc Natl Acad Sci USA **102:** 933–938

Dudareva N, Klempien A, Muhlemann JK, Kaplan I (2013) Biosynthesis, function and metabolic engineering of plant volatile organic compounds. New Phytol **198:** 16–32

Ehlting B, Dluzniewska P, Dietrich H, Selle A, Teuber M, Hänsch R, Nehls U, Polle A, Schnitzler JP, Rennenberg H, et al (2007) Interaction of nitrogen nutrition and salinity in grey poplar (*Populus tremula* × *alba*). Plant Cell Environ **30:** 796–811

Enfissi EM, Fraser PD, Lois LM, Boronat A, Schuch W, Bramley PM (2005) Metabolic engineering of the mevalonate and non-mevalonate isopentenyl diphosphate-forming pathways for the production of health-promoting isoprenoids in tomato. Plant Biotechnol J **3:** 17–27

Estévez JM, Cantero A, Reindl A, Reichler S, León P (2001) 1-Deoxy-D-xylulose-5-phosphate synthase, a limiting enzyme for plastidic isoprenoid biosynthesis in plants. J Biol Chem **276:** 22901–22909

Fuentes J, Lerdau M, Atkinson R, Baldocchi D, Bottenheim J, Ciccioli P, Lamb B, Geron C, Gu L, Guenther A, et al (2000) Biogenic hydrocarbons in the atmospheric boundary layer: a review. Bull Am Meteorol Soc **81:** 1537–1575

Gerber E, Hemmerlin A, Hartmann M, Heintz D, Hartmann MA, Mutterer J, Rodríguez-Concepción M, Boronat A, Van Dorsselaer A, Rohmer M, et al (2009) The plastidial 2-C-methyl-D-erythritol 4-phosphate pathway provides the isoprenyl moiety for protein geranylgeranylation in tobacco BY-2 cells. Plant Cell **21:** 285–300

Gershenzon J, Dudareva N (2007) The function of terpene natural products in the natural world. Nat Chem Biol **3:** 408–414

Ghirardo A, Gutknecht J, Zimmer I, Brüggemann N, Schnitzler JP (2011) Biogenic volatile organic compound and respiratory CO_2 emissions after ^{13}C-labeling: online tracing of C translocation dynamics in poplar plants. PLoS ONE **6:** e17393

Ghirardo A, Koch K, Taipale R, Zimmer I, Schnitzler JP, Rinne J (2010a) Determination of de novo and pool emissions of terpenes from four common boreal/alpine trees by $^{13}CO_2$ labelling and PTR-MS analysis. Plant Cell Environ **33:** 781–792

Ghirardo A, Zimmer I, Brüggemann N, Schnitzler JP (2010b) Analysis of 1-deoxy-D-xylulose 5-phosphate synthase activity in grey poplar leaves using isotope ratio mass spectrometry. Phytochemistry **71:** 918–922

Giuliano G, Tavazza R, Diretto G, Beyer P, Taylor MA (2008) Metabolic engineering of carotenoid biosynthesis in plants. Trends Biotechnol **26:** 139–145

Guenther A (2013) Upscaling biogenic volatile compound emissions from leaves to landscapes. *In* Ü Niinemets, RK Monson, eds, Biology, Controls and Models of Tree Volatile Organic Compound Emissions. Springer, Berlin, pp 391–414

Guevara-García A, San Román C, Arroyo A, Cortés ME, de la Luz Gutiérrez-Nava M, León P, Leon P (2005) Characterization of the *Arabidopsis clb6* mutant illustrates the importance of posttranscriptional regulation of the methyl-D-erythritol 4-phosphate pathway. Plant Cell **17:** 628–643

Hemmerlin A, Hoeffler JF, Meyer O, Tritsch D, Kagan IA, Grosdemange-Billiard C, Rohmer M, Bach TJ (2003) Cross-talk between the cytosolic mevalonate and the plastidial methylerythritol phosphate pathways in tobacco bright yellow-2 cells. J Biol Chem **278:** 26666–26676

Illarionova V, Kaiser J, Ostrozhenkova E, Bacher A, Fischer M, Eisenreich W, Rohdich F (2006) Nonmevalonate terpene biosynthesis enzymes as antiinfective drug targets: substrate synthesis and high-throughput screening methods. J Org Chem **71:** 8824–8834

Ivanova LA, Ronzhina DA, Ivanov LA, Stroukova LV, Peuke AD, Rennenberg H (2009) Chloroplast parameters differ in wild type and transgenic poplars overexpressing *gsh1* in the cytosol. Plant Biol (Stuttg) **11:** 625–630

Kaling M, Kanawati B, Ghirardo A, Albert A, Winkler JB, Heller W, Barta C, Loreto F, Schmitt-Kopplin P, Schnitzler J-P (2014) UV-SI: UV-B mediated metabolic rearrangements in poplar revealed by non-targeted metabolomics. Plant Cell Environ http://dx.doi.org/10.1111/pce.12348

Karl T, Fall R, Rosenstiel TN, Prazeller P, Larsen B, Seufert G, Lindinger W (2002) On-line analysis of the $^{13}CO_2$ labeling of leaf isoprene suggests multiple subcellular origins of isoprene precursors. Planta **215:** 894–905

Kasahara H, Hanada A, Kuzuyama T, Takagi M, Kamiya Y, Yamaguchi S (2002) Contribution of the mevalonate and methylerythritol phosphate pathways to the biosynthesis of gibberellins in Arabidopsis. J Biol Chem **277:** 45188–45194

Kiendler-Scharr A, Andres S, Bachner M, Behnke K, Broch S, Hofzumahaus A, Holland F, Kleist E, et al (2012) Isoprene in poplar emissions: effects on new particle formation and OH concentrations. Atmos Chem Phys **12:** 1021–1030

Kreuzwieser J, Graus M, Wisthaler A, Hansel A, Rennenberg H, Schnitzler JP (2002) Xylem-transported glucose as an additional carbon source for leaf isoprene formation in *Quercus robur*. New Phytol **156:** 171–178

Lange BM, Wildung MR, McCaskill D, Croteau R (1998) A family of transketolases that directs isoprenoid biosynthesis via a mevalonate-independent pathway. Proc Natl Acad Sci USA **95:** 2100–2104

Laule O, Fürholz A, Chang HS, Zhu T, Wang X, Heifetz PB, Gruissem W, Lange M (2003) Crosstalk between cytosolic and plastidial pathways of isoprenoid biosynthesis in *Arabidopsis thaliana*. Proc Natl Acad Sci USA **100:** 6866–6871

Li Z, Sharkey T (2013a) Molecular and pathway controls on biogenic volatile organic compound emissions. *In* Ü Niinemets, RK Monson, eds, Biology, Controls and Models of Tree Volatile Organic Compound Emissions. Springer, Berlin, pp 119–151

Li Z, Sharkey TD (2013b) Metabolic profiling of the methylerythritol phosphate pathway reveals the source of post-illumination isoprene burst from leaves. Plant Cell Environ **36:** 429–437

Lois LM, Rodríguez-Concepción M, Gallego F, Campos N, Boronat A (2000) Carotenoid biosynthesis during tomato fruit development: regulatory role of 1-deoxy-D-xylulose 5-phosphate synthase. Plant J **22:** 503–513

Loivamäki M, Louis S, Cinege G, Zimmer I, Fischbach RJ, Schnitzler JP (2007) Circadian rhythms of isoprene biosynthesis in grey poplar leaves. Plant Physiol **143:** 540–551

Loreto F, Ciccioli P, Brancaleoni E, Frattoni M, Delfine S (2000) Incomplete ^{13}C labelling of α-pinene content of *Quercus ilex* leaves and appearance of unlabelled C in α-pinene emission in the dark. Plant Cell Environ **23:** 229–234

Loreto F, Pinelli P, Brancaleoni E, Ciccioli P (2004) ^{13}C labeling reveals chloroplastic and extrachloroplastic pools of dimethylallyl pyrophosphate and their contribution to isoprene formation. Plant Physiol **135:** 1903–1907

Loreto F, Schnitzler JP (2010) Abiotic stresses and induced BVOCs. Trends Plant Sci **15:** 154–166

Loreto F, Velikova V (2001) Isoprene produced by leaves protects the photosynthetic apparatus against ozone damage, quenches ozone products, and reduces lipid peroxidation of cellular membranes. Plant Physiol **127:** 1781–1787

Mayrhofer S, Teuber M, Zimmer I, Louis S, Fischbach RJ, Schnitzler JP (2005) Diurnal and seasonal variation of isoprene biosynthesis-related genes in grey poplar leaves. Plant Physiol **139:** 474–484

Mongélard G, Seemann M, Boisson AM, Rohmer M, Bligny R, Rivasseau C (2011) Measurement of carbon flux through the MEP pathway for isoprenoid synthesis by ^{31}P-NMR spectroscopy after specific inhibition of 2-C-methyl-D-erythritol 2,4-cyclodiphosphate reductase: effect of light and temperature. Plant Cell Environ **34:** 1241–1247

Monson RK, Grote R, Niinemets Ü, Schnitzler JP (2012) Modeling the isoprene emission rate from leaves. New Phytol **195:** 541–559

Moses T, Pollier J, Thevelein JM, Goossens A (2013) Bioengineering of plant (tri)terpenoids: from metabolic engineering of plants to synthetic biology in vivo and in vitro. New Phytol **200:** 27–43

Muñoz-Bertomeu J, Arrillaga I, Ros R, Segura J (2006) Up-regulation of 1-deoxy-D-xylulose-5-phosphate synthase enhances production of essential oils in transgenic spike lavender. Plant Physiol **142:** 890–900

Niinemets Ü, Monson RK (2013) State-of-the-art of BVOC research: what do we have and what have we missed? *In* Ü Niinemets, RK Monson, eds, Biology, Controls and Models of Tree Volatile Organic Compound Emissions. Springer, Berlin, pp 95–118

Niinemets U, Tenhunen JD, Harley PC, Steinbrecher R (1999) A model of isoprene emission based on energetic requirements for isoprene synthesis and leaf photosynthetic properties for *Liquidambar* and *Quercus*. Plant Cell Environ **22:** 1319–1335

Peñuelas J, Llusià J, Asensio D, Munné-Bosch S (2005) Linking isoprene with plant thermotolerance, antioxidants and monoterpene emissions. Plant Cell Environ **28:** 278–286

Poisson N, Kanakidou M, Crutzen PJ (2000) Impact of non-methane hydrocarbons on tropospheric chemistry and the oxidizing power of the global troposphere: 3-dimensional modelling results. J Atmos Chem **36:** 157–230

Pulido P, Toledo-Ortiz G, Phillips MA, Wright LP, Rodríguez-Concepción M (2013) *Arabidopsis* J-protein J20 delivers the first enzyme of the plastidial isoprenoid pathway to protein quality control. Plant Cell **25:** 4183–4194

Rasulov B, Bichele I, Laisk A, Niinemets Ü (2013) Competition between isoprene emission and pigments synthesis during leaf development in aspen. Plant Cell Environ **37:** 724–741

Rasulov B, Copolovici L, Laisk A, Niinemets U (2009a) Postillumination isoprene emission: in vivo measurements of dimethylallyldiphosphate pool size and isoprene synthase kinetics in aspen leaves. Plant Physiol **149:** 1609–1618

Rasulov B, Hüve K, Bichele I, Laisk A, Niinemets Ü (2010) Temperature response of isoprene emission in vivo reflects a combined effect of substrate limitations and isoprene synthase activity: a kinetic analysis. Plant Physiol **154:** 1558–1570

Rasulov B, Hüve K, Välbe M, Laisk A, Niinemets U (2009b) Evidence that light, carbon dioxide, and oxygen dependencies of leaf isoprene emission are driven by energy status in hybrid aspen. Plant Physiol **151:** 448–460

Rios-Estepa R, Lange BM (2007) Experimental and mathematical approaches to modeling plant metabolic networks. Phytochemistry **68:** 2351–2374

Rodríguez-Concepción M (2006) Early steps in isoprenoid biosynthesis: multilevel regulation of the supply of common precursors in plant cells. Phytochem Rev **5:** 1–15

Rosenstiel TN, Potosnak MJ, Griffin KL, Fall R, Monson RK (2003) Increased CO_2 uncouples growth from isoprene emission in an agriforest ecosystem. Nature **421:** 256–259

Ryan AC, Hewitt CN, Possell M, Vickers CE, Purnell A, Mullineaux PM, Davies WJ, Dodd IC (2014) Isoprene emission protects photosynthesis but reduces plant productivity during drought in transgenic tobacco (*Nicotiana tabacum*) plants. New Phytol **201:** 205–216

Schnitzler JP, Graus M, Kreuzwieser J, Heizmann U, Rennenberg H, Wisthaler A, Hansel A (2004) Contribution of different carbon sources to isoprene biosynthesis in poplar leaves. Plant Physiol **135:** 152–160

Schnitzler JP, Louis S, Behnke K, Loivamäki M (2010) Poplar volatiles: biosynthesis, regulation and (eco)physiology of isoprene and stress-induced isoprenoids. Plant Biol (Stuttg) **12:** 302–316

Schnitzler JP, Zimmer I, Bachl A, Arend M, Fromm J, Fischbach RJ (2005) Biochemical properties of isoprene synthase in poplar (*Populus* × *canescens*). Planta **222:** 777–786

Sharkey TD (1995) Why plants emits isoprene. Nature **374:** 769

Sharkey TD, Wiberley AE, Donohue AR (2008) Isoprene emission from plants: why and how. Ann Bot (Lond) **101:** 5–18

Sharkey TD, Yeh S (2001) Isoprene emission from plants. Annu Rev Plant Physiol Plant Mol Biol **52:** 407–436

Sun Z, Hüve K, Vislap V, Niinemets U (2013a) Elevated [CO_2] magnifies isoprene emissions under heat and improves thermal resistance in hybrid aspen. J Exp Bot **64:** 5509–5523

Sun Z, Niinemets Ü, Hüve K, Noe SM, Rasulov B, Copolovici L, Vislap V (2012) Enhanced isoprene emission capacity and altered light responsiveness in aspen grown under elevated atmospheric CO_2 concentration. Glob Change Biol **18:** 3423–3440

Sun Z, Niinemets U, Hüve K, Rasulov B, Noe SM (2013b) Elevated atmospheric CO_2 concentration leads to increased whole-plant isoprene emission in hybrid aspen (*Populus tremula* × *Populus tremuloides*). New Phytol **198:** 788–800

Thulasiram HV, Erickson HK, Poulter CD (2007) Chimeras of two isoprenoid synthases catalyze all four coupling reactions in isoprenoid biosynthesis. Science **316:** 73–76

Trowbridge AM, Asensio D, Eller ASD, Way DA, Wilkinson MJ, Schnitzler JP, Jackson RB, Monson RK (2012) Contribution of various carbon sources toward isoprene biosynthesis in poplar leaves mediated by altered atmospheric CO_2 concentrations. PLoS ONE **7:** e32387

Velikova V, Ghirardo A, Vanzo E, Merl J, Hauck SM, Schnitzler JP (January 22, 2014) The genetic manipulation of isoprene emissions in poplar plants remodels the chloroplast proteome. J Proteome Res http://dx.doi.org/10.1021/pr401124z

Velikova V, Loreto F (2005) On the relationship between isoprene emission and thermotolerance in *Phragmites australis* leaves exposed to high temperatures and during the recovery from a heat stress. Plant Cell Environ **28:** 318–327

Vickers CE, Gershenzon J, Lerdau MT, Loreto F (2009) A unified mechanism of action for volatile isoprenoids in plant abiotic stress. Nat Chem Biol **5:** 283–291

Vranová E, Coman D, Gruissem W (2012) Structure and dynamics of the isoprenoid pathway network. Mol Plant **5:** 318–333

Way DA, Ghirardo A, Kanawati B, Esperschütz J, Monson RK, Jackson RB, Schmitt-Kopplin P, Schnitzler JP (2013) Increasing atmospheric CO_2 reduces metabolic and physiological differences between isoprene- and non-isoprene-emitting poplars. New Phytol **200:** 534–546

Way DA, Schnitzler JP, Monson RK, Jackson RB (2011) Enhanced isoprene-related tolerance of heat- and light-stressed photosynthesis at low, but not high, CO_2 concentrations. Oecologia **166:** 273–282

Weise SE, Li Z, Sutter AE, Corrion A, Banerjee A, Sharkey TD (2013) Measuring dimethylallyl diphosphate available for isoprene synthesis. Anal Biochem **435:** 27–34

Werner RA, Brand WA (2001) Referencing strategies and techniques in stable isotope ratio analysis. Rapid Commun Mass Spectrom **15:** 501–519

Wiberley AE, Donohue AR, Westphal MM, Sharkey TD (2009) Regulation of isoprene emission from poplar leaves throughout a day. Plant Cell Environ **32:** 939–947

Wolfertz M, Sharkey TD, Boland W, Kühnemann F (2004) Rapid regulation of the methylerythritol 4-phosphate pathway during isoprene synthesis. Plant Physiol **135:** 1939–1945

Wu S, Schalk M, Clark A, Miles RB, Coates R, Chappell J (2006) Redirection of cytosolic or plastidic isoprenoid precursors elevates terpene production in plants. Nat Biotechnol **24:** 1441–1447

Xiao Y, Savchenko T, Baidoo EEK, Chehab WE, Hayden DM, Tolstikov V, Corwin JA, Kliebenstein DJ, Keasling JD, Dehesh K (2012) Retrograde signaling by the plastidial metabolite MEcPP regulates expression of nuclear stress-response genes. Cell **149:** 1525–1535

Zeidler JG, Lichtenthaler HL, May HU, Lichtenthaler FW (1997) Is isoprene emitted by plants synthesized via the novel isopentenyl pyrophosphate pathway? Z Naturforsch C **53:** 980–986

Zhou C, Li Z, Wiberley-Bradford AE, Weise SE, Sharkey TD (2013) Isopentenyl diphosphate and dimethylallyl diphosphate/isopentenyl diphosphate ratio measured with recombinant isopentenyl diphosphate isomerase and isoprene synthase. Anal Biochem **440:** 130–136

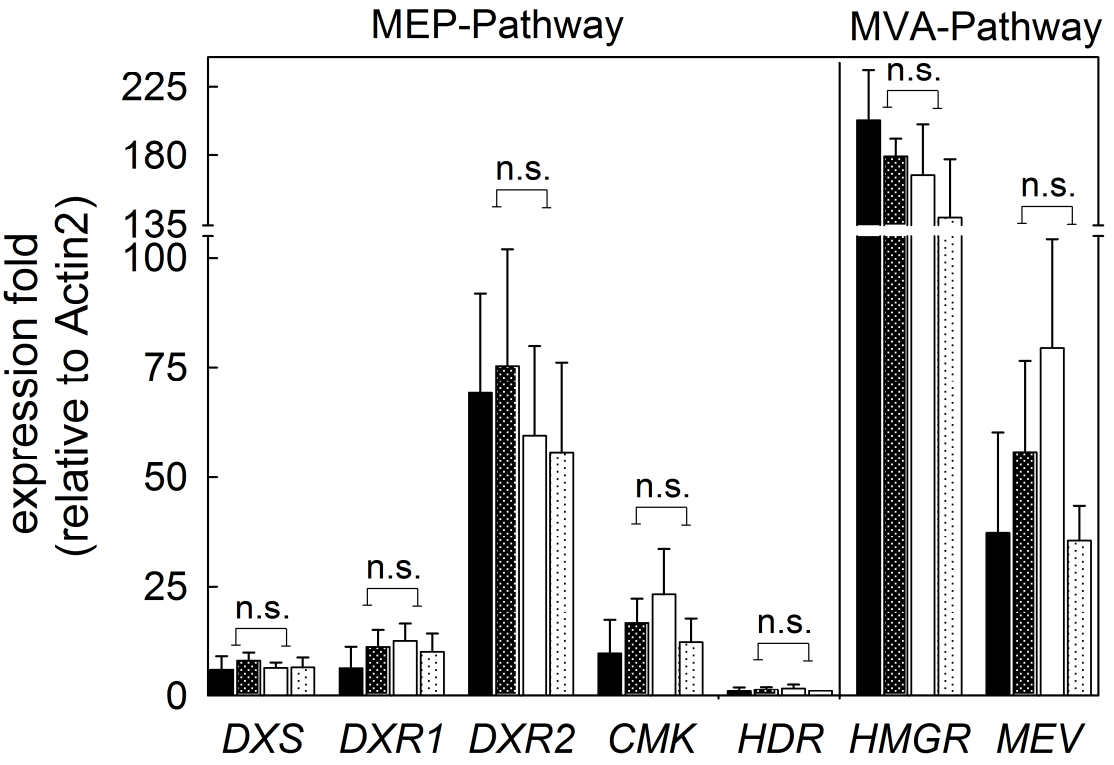

Figure S1.

Transcripts levels of the genes on methylerythritol 4-phosphate (MEP)-pathway (*PcDXS, PcDXR1, PcDXR2, PcCMK, PcHDR*) and mevalonate pathway (*PcHMGR, PcMEV*) in isoprene-emitting (IE: wild-type = ■, empty vector = ▩) and isoprene non-emitting (NE: RA1 = □ , RA2 = ▨) leaves of *Populus* x *canescens.* Ninth leaves from the apex were subjected to 1000 μmol m^{-2} s^{-1} of incident photosynthetically active quantum flux density (PPFD), 30°C of leaf temperature and 380 μmol mol^{-1} of CO_2 for 60 min before taking the samples. The expression is shown relative to the housekeeping gene Actin 2. Means values for five independent biological replicates ± SE are demonstrated. Significant differences between the IE and NE were tested by one-way ANOVA at $P < 0.05$. n.s.= not significant.

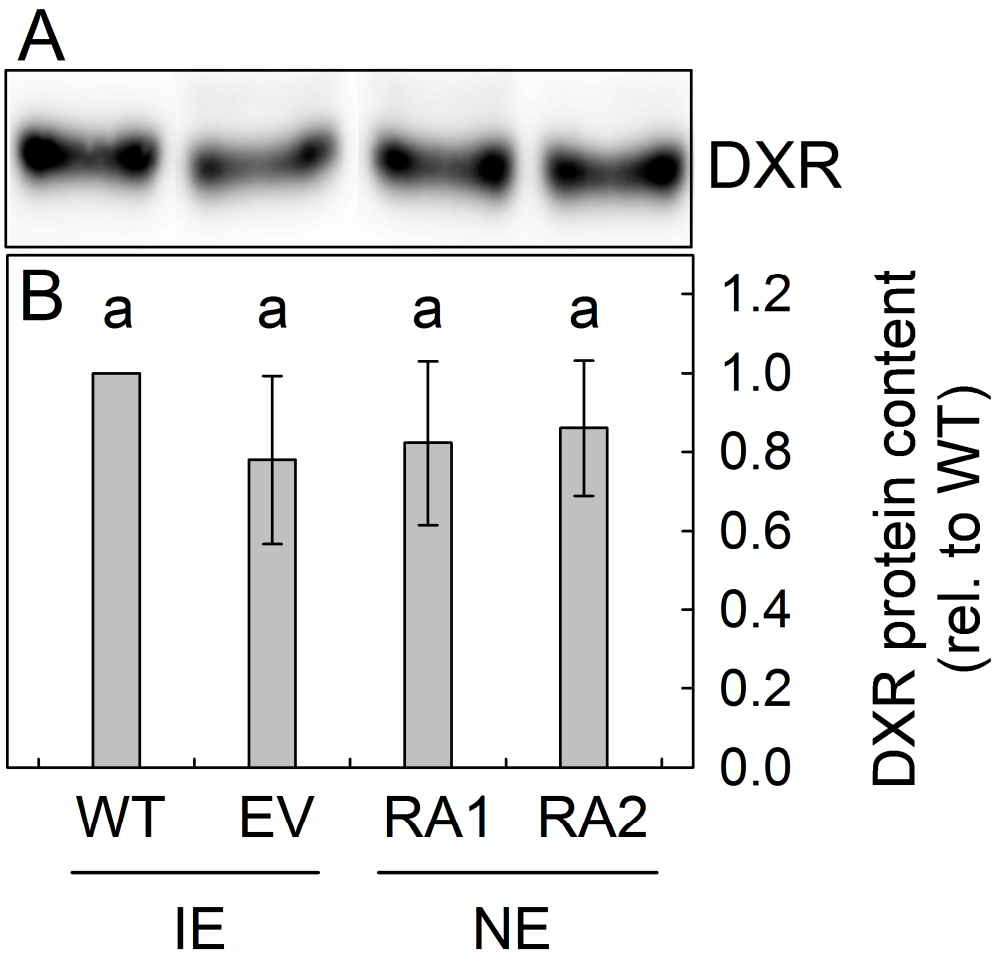

Figure S2.

(**A**) Representative image of immunoblot analyses of PcDXR protein (51 kDa) content and (**B**) quantitative data of PcDXR protein content relative to WT plants. Means of n = 4 ± SE are demonstrated. Significance differences (two-way ANOVA followed by Tukey`s test) at $P < 0.05$ are indicated with different letters.